ACS Partner Journal
PRECISION CHEMISTRY
pubs.acs.org/PrecisionChem

Review

The Trend of Nonenzymatic Nucleic Acid Amplification: Strategies and Diagnostic Application

Published as part of Precision Chemistry special issue "Precision Diagnostics".

Junyou Li,[#] Ting Li,[#] Zheng Zou,[#] and Hung-Wing Li*

Cite This: *Precis. Chem.* 2025, 3, 187−205

Read Online

ACCESS | Metrics & More | Article Recommendations

ABSTRACT: Nonenzymatic nucleic acid amplification reactions, especially nonenzymatic DNA amplification reactions (NDARs), are thermodynamically driven processes that operate without enzymes, relying on toehold-mediated strand displacement (TMSD) and branch migration. With their sensitive and efficient signal amplification capabilities, NDARs have become essential tools for biomarker detection and intracellular imaging. They encompass four primary amplification methods: catalytic hairpin assembly (CHA), hybridization chain reaction (HCR), DNAzyme-based amplification, and entropy-driven circuits (EDC). Based on amplification mechanisms, NDARs can be categorized into three types: stimuli-responsive NDARs, which employ single amplification strategies triggered by specific stimuli like pH, light, or biomolecules; cascade NDARs, which integrate two or more amplification reactions for stepwise signal enhancement; and autocatalytic NDARs, which achieve exponential amplification through self-sustained cycling. These advanced designs progressively improve amplification efficiency, enhance sensitivity, and minimize background noise, enabling precise detection of proteins, viruses, and nucleic acids as well as applications in cancer cell imaging and therapy. Compared with classical NDARs, these approaches significantly reduce signal leakage, offering broader applicability in diagnostics, imaging, and therapeutic contexts. This review summarizes recent advancements, addresses existing challenges, and explores future directions, providing insights into the development and applications of NDARs.

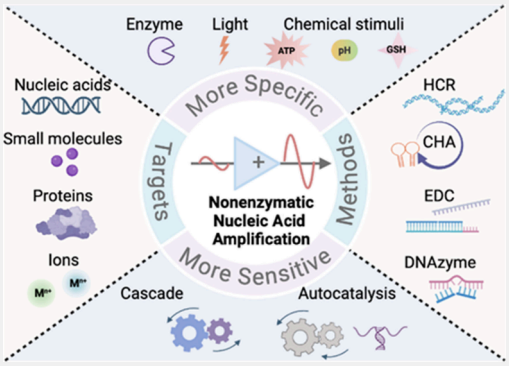

KEYWORDS: *nonenzymatic DNA amplification reaction, biomarkers detection, stimuli-responsive, cascade, autocatalytic, enhanced sensitivity, precise detection, cell imaging*

INTRODUCTION

Intracellular molecules such as RNA and proteins play critical roles in regulating cellular activities, including division, proliferation, and migration.[1] Abnormal expression and dysfunction of these molecules are often associated with the onset and progression of various diseases. Disease-related molecules, referred to as biomarkers, are typically found in liquid biopsies such as plasma, serum, saliva, urine, or pleural effusions, as well as in specific tissues depending on the disease's nature. The detection of these biomarkers is crucial for understanding disease mechanisms and facilitating the development of personalized precision medicine, particularly for early stage disease diagnosis and tailored treatment strategies.[2]

Deoxyribonucleic acid (DNA), beyond its role as the carrier of genetic information, has emerged as a versatile material for designing diagnostic tools due to its biocompatibility, programmability, and ease of synthesis.[3] Over the years, a variety of DNA-based probes have been developed to detect a wide range of analytes, including nucleic acids (NAs), proteins, and small molecules.[4−7] However, the detection of biomarkers in biological environments is often challenging due to their low abundance and the complexity of the surrounding physiological conditions. To overcome these challenges, signal amplification strategies are essential for enhancing sensitivity and lowering detection limits in diagnostic applications.[8]

Signal amplification systems can be broadly categorized into enzymatic and nonenzymatic approaches. Enzymatic amplification methods, such as polymerase chain reaction (PCR), rolling circle amplification (RCA), and loop-mediated isothermal amplification (LAMP), utilize enzymes like polymerases to achieve detection of trace analytes.[9,10] Despite their widespread use, these enzymatic techniques have significant limitations. They require strictly controlled reaction conditions such as specific temperature ranges, cofactors, or ionic environments,

Received: December 19, 2024
Revised: February 18, 2025
Accepted: February 19, 2025
Published: March 3, 2025

https://doi.org/10.1021/prechem.4c00100
Precis. Chem. 2025, 3, 187−205

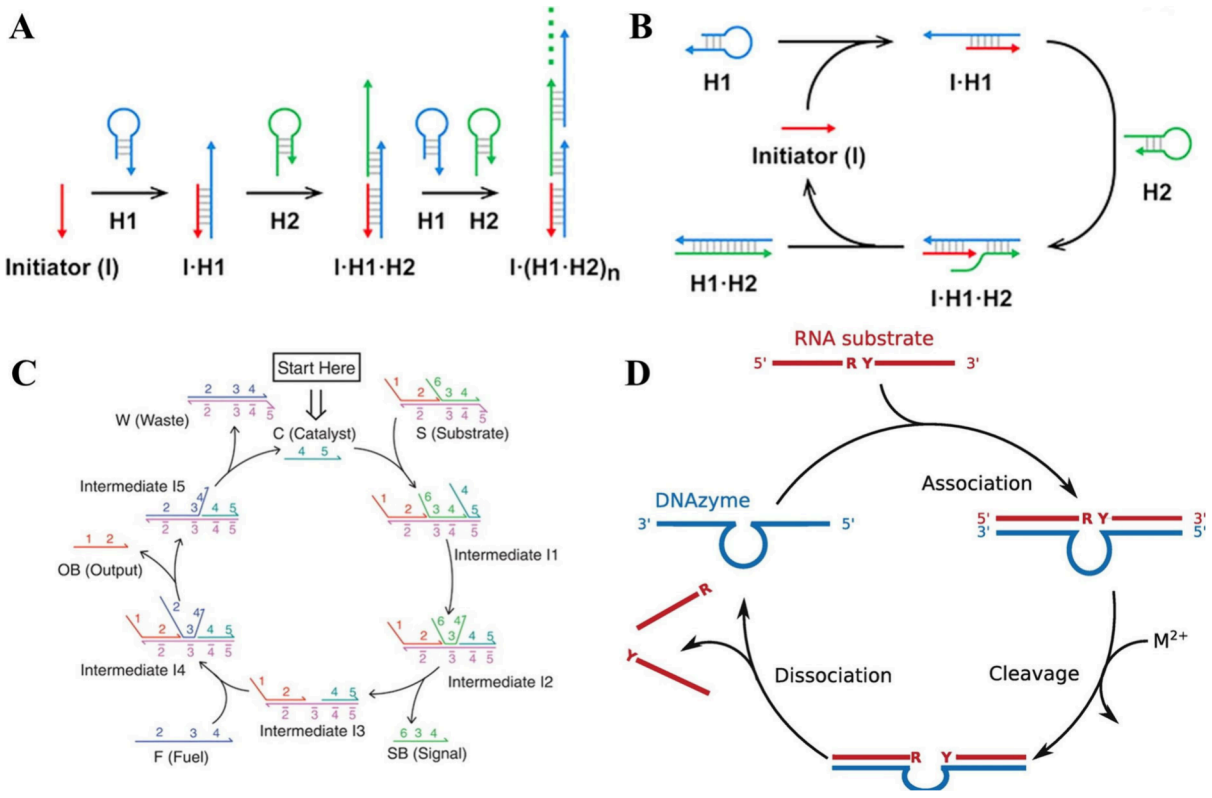

Figure 1. Reaction mechanism of four classic NDARs. (A) The reaction mechanism of the hybridization chain reaction. Reproduced with permission under the terms of the Creative Commons Attribution License (CC BY) from ref 23. Copyright 2023, Mo et al. (B) The reaction mechanism of the catalytic hairpin assembly. Reproduced with permission under the terms CC BY from ref 23. Copyright 2023, Mo et al. (C) The reaction mechanism of the entropy-driven DNA reaction. Reproduced with permission from ref 25. Copyright 2007, The American Association for the Advancement of Science. (D) The reaction mechanism of DNAzymes. Reproduced with permission from ref 27. Copyright 2022, Gerhard Steger et al.

which make them unsuitable for in vivo applications. Additionally, the high cost of engineered enzymes, along with the challenges associated with their storage and transportation, further restricts their practical application.

In contrast, nonenzymatic DNA amplification reactions (NDARs) have emerged as promising alternatives, providing significant value for developing low-cost and robust point-of-care testing (POCT).[11] These reactions rely on thermodynamic principles, such as toehold-mediated strand displacement (TMSD) and branch migration, to achieve signal amplification without the need for protein enzymes. Typically, NDARs involve a DNA double-stranded complex with a single-stranded "toehold" region and a single-stranded DNA that hybridizes with the toehold to trigger a strand displacement reaction. This process leads to the formation of a more thermodynamically stable double-stranded product.[12,13] Foundational NDAR strategies include the hybridization chain reaction (HCR), catalytic hairpin assembly (CHA), entropy-driven catalysis (EDC), and DNAzyme-based approaches. These strategies have been widely applied for detecting various biomarkers, including NAs, small molecules, proteins, exosomes, and even whole cells.[14−17]

While previous reviews have summarized the principles and applications of NDARs,[18−20] they often adopt a scope that focuses on a single detection method, analyte, or signal output format. Furthermore, recent advancements in NDAR technology, such as stimuli-responsive designs and cascade amplification systems, have not been thoroughly explored. This review aims to bridge these gaps by providing a holistic overview of classic and advanced NDAR strategies, emphasizing their mechanisms and applications. Particular attention is given to stimuli-responsive NDAR systems, which allow for dynamic and programmable detection, and cascade amplification NDAR systems, which significantly enhance detection sensitivity. Finally, the challenges and future prospects of NDARs in diagnostic and imaging applications are discussed.

THE REACTION MECHANISM OF CLASSIC NDARS

NDARs have been developed to achieve varying degrees of signal amplification, categorized as linear, square, or exponential amplification systems based on the rate of signal growth over time.[11,21] The most widely studied NDARs are based on four fundamental mechanisms: Hybridization Chain Reaction (HCR), Catalytic Hairpin Assembly (CHA), Entropy-Driven Catalysis (EDC), and DNAzyme-Based Amplification. Each of these mechanisms offers unique advantages for amplifying signals in biomarker detection applications,[22] and they are introduced in the following text.

HCR and CHA enable continuous signal amplification (Figure 1A, 1B). Both strategies utilize two hairpin DNA probes, H1 and H2. In the presence of initiator (I), I binds to the toehold of H1, gradually opening its stem-loop structure. Subsequently, H2 binds to the remaining single strand of the opened H1, opening its stem-loop structure. The key difference between HCR and CHA is whether they remain in the final products after H2 and H1 hybridization. In HCR, I remains bound to H1, and the opened H2 continues to open new H1 molecules, eventually forming a long double-stranded DNA with hundreds of repeating units until H1 and H2 are exhausted. The

https://doi.org/10.1021/prechem.4c00100
Precis. Chem. 2025, 3, 187−205

Table 1. Comparison of Different NDAR Detection Performances

NDAR type	Reaction	Number of reactants	Analyte	LOD	Time	ref
Stimuli-response NDARs	pH-response	8	miRNA-21, miRNA-155	1.46 pM, 0.72 pM	1.5 h	31
	pH-response	4	DNA	38 pM	70 min	33
	pH-response	5	miRNA-21	0.2 pM	2 h	34
	ATP-response	4	miRNA-21	17 pM	2 h	38
	ATP-response	3	miRNA-155	52.7 pM	\	39
	ATP-response	5	miRNA-221	0.19 pM	1 h	40
	GSH-response	5	miRNA-21	6 pM	8 h	42
	Light-response	3	miRNA-133a	36.12 aM	3 h	48
	Multistimuli-response	3	miRNA-21	pM level	1 h	49
	Multistimuli-response	4	miRNA-21	0.07 nM/0.43 fM (optical/electrochemical)	90 min/40 min	50
Cascade NDARs	CHA-HCR	4	miRNA-199a	24.1 aM	130 min	58
	CHA-DNAzyme	5	Uracil DNA glycosylase	0.23 mU/mL	1 h	65
	HCR-HCR	7	miRNA-21	3 pM	2 h	67
	HCR-EDC	6	DNA	87 fM	45 min	68
	HCR-DNAzyme	7	lipoprotein	10 mg/dL (HDL)/30 mg/dL (LDL)	1 h	69
	EDC-CHA	8	DNA	15.6 fM	1 h	71
	EDC-HCR	6	DNA	7 pM	45 min	72
	DNAzyme-CHA	7	*E. coli*	50 cells/mL	85 min	74
	DNAzyme-HCR	3	alpha-fetoprotein	15.8 fg/mL	90 min	78
	Multilayer	4	miRNA-21	162 fM	4 h	80
Autocatalytic NDARs	HCR based	4	miRNA-21	0.6 pM	3 h	93
	CHA based	4	miRNA-21	1.7 pM	3 h	92
	HCR-CHA	7	miRNA-21	0.5 pM	3 h	95
	HCR-CHA	7	Polynucleotide Kinase	2.98×10^{-4} U/mL	3 h	89
	HCR-CHA	6	DNA Methyltransferase	0.011 U/mL	2.5 h	90
	HCR-HCR	7	Polynucleotide Kinase	2.82×10^{-4} U/mL	160 min	88
	HCR-HCR	6	miRNA-21	0.1 pM	5 h	94
	HCR-DNAzyme	5	miRNA-21	3 pM	3 h	91
	CHA-DNAzyme	6	miRNA-21	0.3 pM	5 h	96
	EDC-DNAzyme	4	miRNA-122	0.075 aM	8 h	85
	EDC-DNAzyme	3	miRNA-21	21 pM	3 h	86
	DNAzyme−DNAzyme	4	DNA sequence	1 pM	14 h	84

I strand in the HCR amplifier remains part of the long double-stranded helix structure without participating in subsequent reactions, categorizing it as a trigger strand displacement amplifier. In contrast, H2 gradually replaces I in CHA and stops elongating after forming a complementary double strand with H1 (Figure 1B). The replaced I cyclically reacts with new H1, opening its hairpin structure and then being replaced by H2. Therefore, CHA is categorized as a catalyst strand displacement amplifier with decreased entropy.[23] HCR and CHA have been widely used in the field of ultralow biomarker detection and bioimaging.[24]

Entropy-driven circuit (EDC), first presented by Zhang et al., in 2007, is an entropy-increased catalyst strand displacement amplifier (Figure 1C).[25] This catalytic circuit utilizes a series of linear single-stranded DNA molecules and is driven forward thermodynamically by the entropic gain of the liberated molecules instead of the enthalpy gain of base-pair formation. In the presence of the target (catalyst C), the substrate (S) is converted to a waste complex (W) with the help of the fuel strand (F), releasing two byproduct strands (SB and OB). The entire system is driven forward by increasing entropy; 2 DNA molecules/complexes (S and F) convert to 3 DNA molecules/complexes (W, SB, and OB), however, the number of base pairs remains unchanged, i.e., domains 2/2*, 3/3*, and 4/4*, are double-stranded before and after the conversion. Figure 1C shows the detailed reaction mechanism, where C first binds with S to form the four-stranded intermediate I1. After branch migration, I1 rearranges to form I2. Then, I2 spontaneously dissociates into SB and I3 due to the weak binding of domains 3. Then F binds to I2 to form I4, which then quickly rearranges to release OB and I5. Finally, C is dissociated and regenerated from I5 by the strand displacement of F. The regenerated C then triggers a new cycle until reactants deplete.

Unlike the above three amplifiers, DNAzymes maintain amplification cycles that are not only based on strand displacement. The amplifiers based on DNAzymes also utilize the cleaving activity of DNAzyme, which plays a catalytic role by continuously cleaving and releasing broken substrate DNA to achieve amplification. DNAzymes are catalytically active DNA sequences capable of cleaving specific substrates in the presence of cofactors such as metal ions.[26] A typical DNAzyme consists of a catalytic core of about 15 nucleotides and two short binding arms of about 10 nucleotides located on either side of the catalytic core, (Figure 1D). A DNAzyme has two binding arms designed to bind to the complementary substrate strand in a Watson−Crick pairing. The DNAzyme binds to its target substrate strand and makes a DNAzyme-substrate complex. The catalytic motif of the DNAzyme then cleaves its target substrate

https://doi.org/10.1021/prechem.4c00100
Precis. Chem. 2025, 3, 187−205

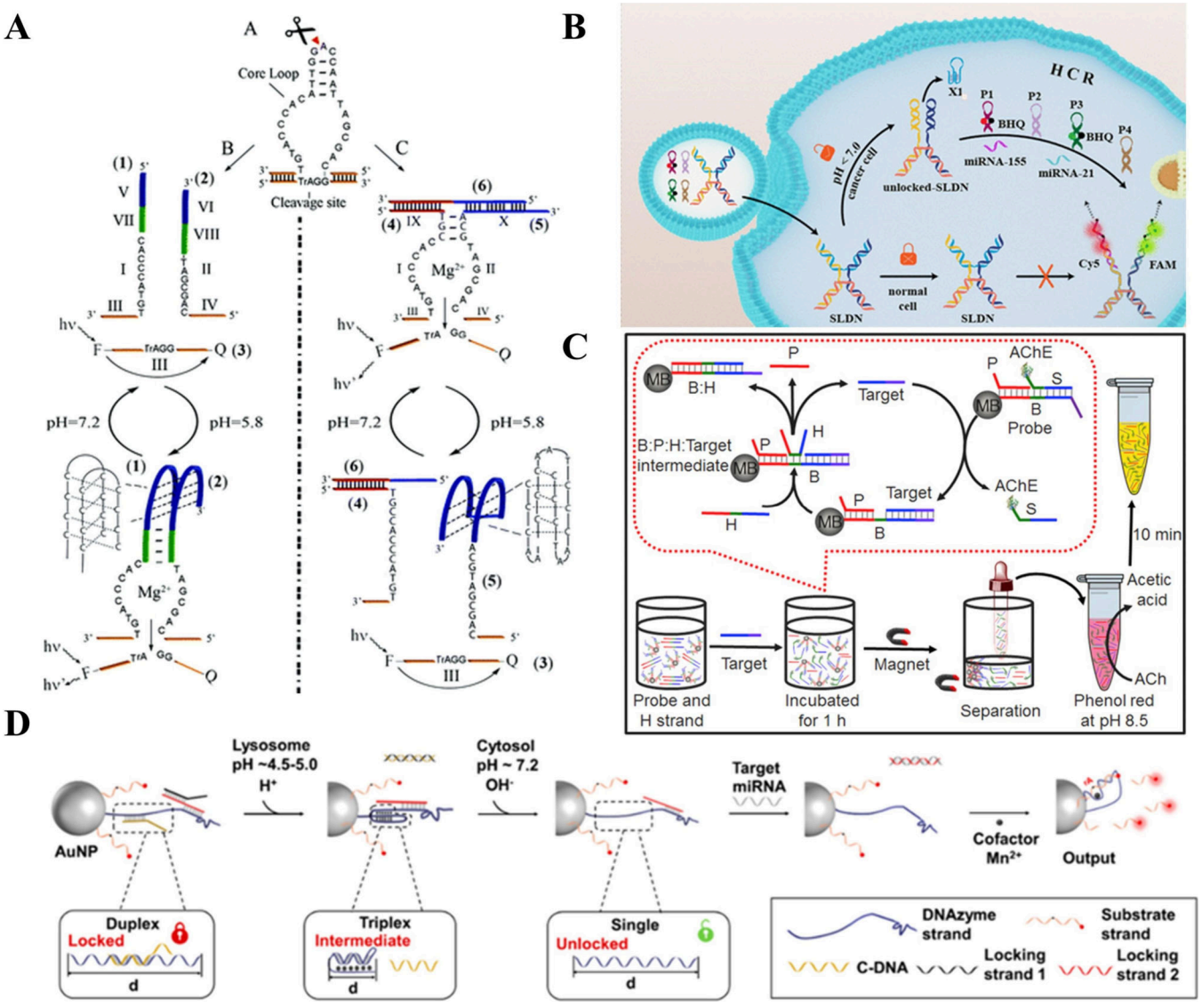

Figure 2. pH-response NDARs. (A) Mechanism of the pH-triggered switchable Mg^{2+}-dependent DNAzyme. Reproduced with permission from ref 30. Copyright 2010 Royal Society of Chemistry. (B) pH-stimulated self-locked DNA nanostructure with HCR for cell imaging. Reproduced with permission from ref 31. Copyright 2023 American Chemical Society. (C) AChE-based colorimetric biosensors for pH detection. Reproduced with permission from ref 33. Copyright 2017 Elsevier. (D) pH-responsive programmable DNA nanomachine on AuNP for targeting miRNA. Reproduced with permission from ref 34. Copyright 2022 American Chemical Society.

into pieces. After cleaving the substrate strand, the DNAzyme becomes free again to enter into the next cycle. It enables sustained catalytic shearing and provides amplified signals by cooperating with the abundant complementary substrate strands.[27]

■ ADVANCED NDAR AND APPLICATIONS IN DIAGNOSIS

Recent advancements in NDAR technology have led to the development of specialized amplification strategies tailored to address specific challenges in sensitivity, specificity, and adaptability. Stimuli-responsive NDARs are designed to activate or modulate amplification processes in response to specific environmental or physiological conditions such as changes in pH, temperature, light, or the presence of specific molecules such as ATP and GSH to trigger precise amplification reactions. Cascade NDARs that leverage sequential reaction steps to achieve amplified detection signals, enabling the detection of ultralow target concentrations with high accuracy, as well as autocatalytic NDARs that introduce self-sustaining amplification mechanisms, where reaction products act as catalysts to perpetuate the process, achieving exponential signal generation and amplification efficiency, address the key limitations of traditional NDAR systems, such as limited amplification efficiency, signal leakage, and suboptimal performance in complex biological environments. By leveraging stimuli-responsiveness, cascade designs, and autocatalytic feedback mechanisms, these NDARs represent a transformative leap in the field, enabling robust applications in precision diagnostics and therapeutic monitoring. This discussion explores the principles, advantages, and challenges associated with stimuli-responsive, cascade, and autocatalytic NDARs, highlighting their potential to revolutionize the fields of molecular biology and medicine. The summary of the NDARs of concern is attached at the end of the discussion as Table 1.

https://doi.org/10.1021/prechem.4c00100
Precis. Chem. 2025, 3, 187−205

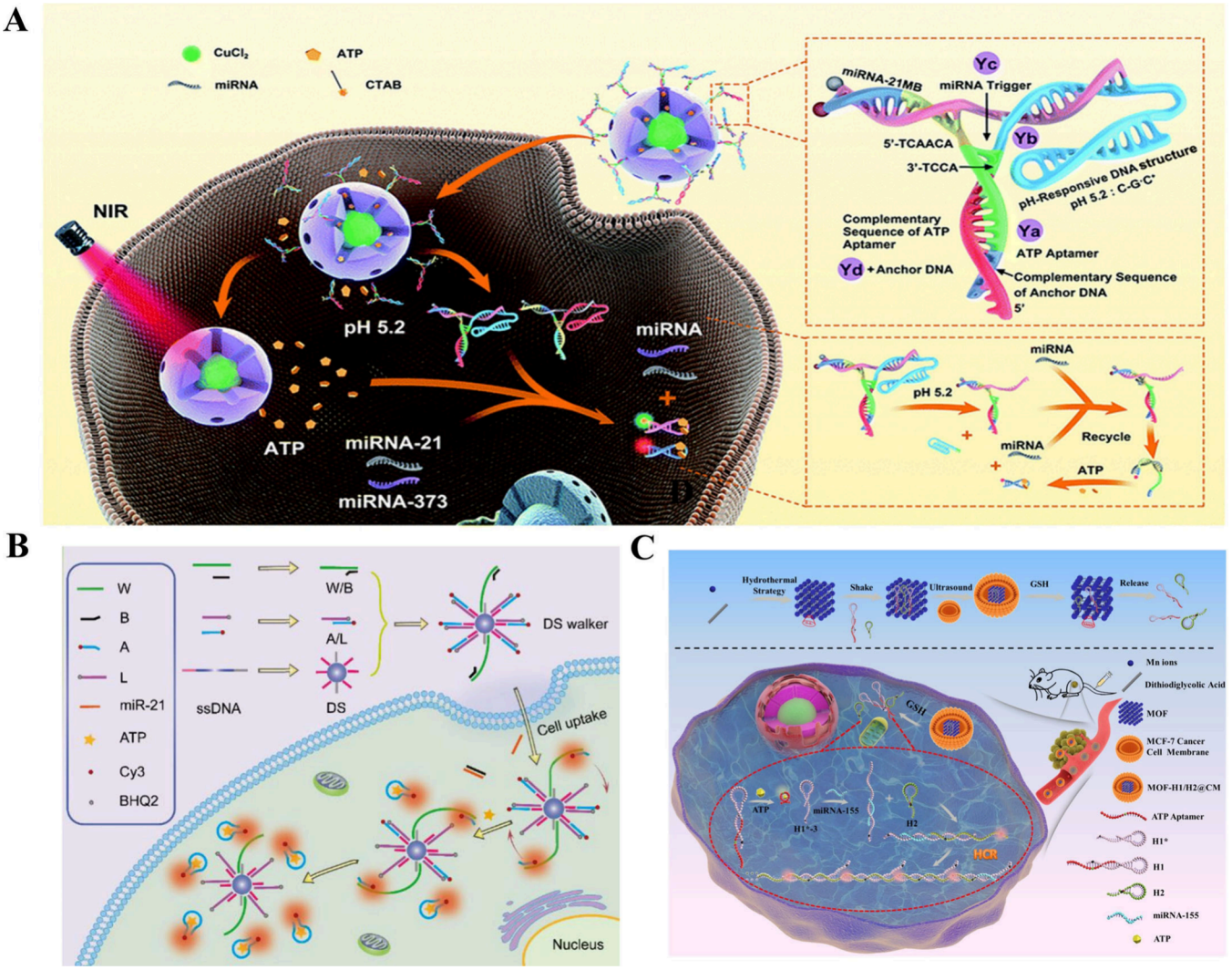

Figure 3. ATP-response NDARs. (A) ATP-self-powered strand-displacement cascade amplification system for miRNA detection. Reproduced with permission from ref 37. Copyright 2017 Royal Society of Chemistry. (B) ATP-powered 3D DNA walker for miRNA-21 detection. Reproduced with permission from ref 38. Copyright 2023 American Chemical Society. (C) ATP aptamer-loaded glutathione-coated tumor cell membrane-responsive metal−organic framework for miRNA-155 cell imaging. Reproduced with permission from ref 39. Copyright 2021 American Chemical Society.

Stimuli-Responsive NDARs

The stimulus-reactive nucleic acid amplification strategy has important application potential in biomedical diagnostics, especially in the context of specific and rapid detection. By limiting amplification to relevant conditions, these systems reduce background noise and false positives, improve the accuracy and reliability of test results, and enable efficient and controllable NDARs for specific external stimuli such as pH, temperature, light, ions, or biomolecules. These stimuli act as triggers that activate or modulate the amplification process, thus adapting NDARs to a specific environmental or physiological context. The design of stimuli-reactive amplification systems typically involves DNA probes, primers, and enzymes that exhibit structural changes or regulation of activity in response to specific stimuli. These changes facilitate the initiation and regulation of NDARs. By combining different NDARs techniques, the amplification effect of the reaction can be further improved. For example, HCR and CHA are particularly well suited for biomolecular triggered amplification attributed to the highly specific target recognition and efficient signal amplification, for ultrasensitive detection of biomarkers even in complex biological samples.[28]

pH-Responsive NDARs. pH-responsive DNA amplification is a specialized approach in DNA amplification, where the amplification process is mainly regulated by pH changes. This technique utilizes the sensitivity of certain DNA structures, enzymes, or other molecular systems to pH variations, making it especially useful in applications where the target environment has a distinct pH, such as cancerous tissues, which are often slightly acidic. pH-responsive DNA amplification can increase specificity, reduce background noise, and enhance detection sensitivity in diagnostics and biosensing.[29]

i-motifs are cytosine-rich sequences that, at acidic pH, fold due to the protonation of cytosine bases to form a four-stranded DNA structure. DNAzyme containing the i-motif can take advantage of this structural change to regulate the activity. When pH drops, i-motif forms and alters the conformation of DNAzyme, activating or inhibiting its catalytic function (Figure 2A).[30] Han et al. proposed a pH-stimulated self-locking DNA nanostructure (SLDN) to enable the differentiation of cancer cells from normal cells as well as sensitive miRNA detection and

https://doi.org/10.1021/prechem.4c00100
Precis. Chem. 2025, 3, 187−205

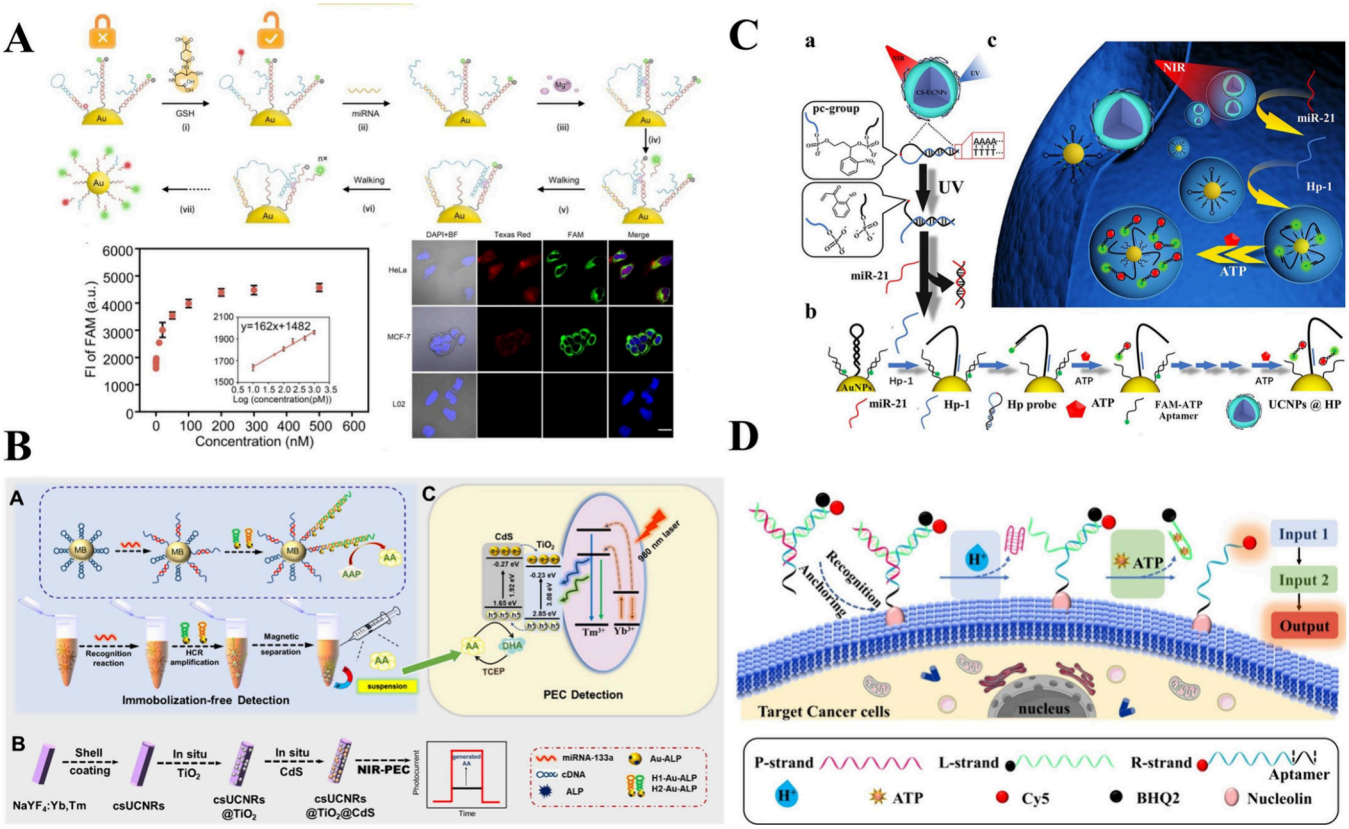

Figure 4. GSH-response, light-response, and multistimuli-response NDARs. (A) GSH-responsive DNAzyme-based nanodevice for miRNA tumor imaging. Reproduced with permission from ref 42. Copyright 2022 Elsevier. (B) NIR-initiated photoelectrochemical biosensor with HCR for miRNA detection. Reproduced with permission from ref 48. Copyright 2021 American Chemical Society. (C) Light-activated 3D DNA walker powered by ATP for miRNA in situ detection. Reproduced with permission from ref 49. Copyright 2021 American Chemical Society. (D) Sequentially responsive aptamer sensor with the "and" logic gate for cancer cell identification. Reproduced with permission from ref 51. Copyright 2024 American Chemical Society.

fluorescent biosensing. As shown in Figure 2B, SLDN consists of four customized single-stranded DNA strands (X1, X2, X3, and X4) in a slightly alkaline environment. Then, in a slightly acidic environment, X1 with the i-motif sequence tends to form a quadruplex structure, detaining from SLDN and restoring the fluorescence signal of Cy3.[31] Chai's team constructed acid-stimulated self-assembled DNA nanonetworks (ASDN) to distinguish cancer cells from normal cells, enabled targeted and sensitive detection of miRNA-221 in cancer cells, and enabled live cell imaging of miRNA-221.[32]

Acetylcholine (ACh) hydrolysis catalyzed by acetylcholinesterase (AChE) is a new method of colorimetric biosensing to detect the pH of the solution. Using phenol red as an indicator, Guo et al. developed colorimetric biosensors for corresponding targets by coupling AChE to different recognition elements. The DNA sequence was coupled with an AChE instrument to perform colorimetric and visual detection. In addition, acetaminophen-conjugated DNA can be introduced into molecular programming to achieve nonenzymatic cascade amplification for highly sensitive detection (Figure 2C).[33]

Notably, some DNA sequences will change their secondary structure response to the change of pH. Chao's group fabricated an intelligent pH-responsive programmable DNA (PRPD) nanomachine to perform multilayer DNA cascades, enabling logically precise biosensing and calculation of intracellular miRNA. As shown in Figure 2D, the PRPD nanomachine was constructed on Au nanoparticle (AuNP) decorated with substrate strands as DNA tracks and the four-stranded DNAzyme walker precursors. The DNAzyme strand was designed to be sensitive to pH variation of ~5.0−7.0 by changing its configuration from linear to triplex. The PRPD nanomachine remained in the locked state until passed through intracellular lysosomes with acidic pH and successfully avoided susceptibility to extracellular target miRNA during delivery into cells and finally achieved the amplified imaging of intracellular target miRNA with fluorescence signal of output.[34]

ATP-Responsive NDARs. Besides being the main energy provider, adenosine triphosphate (ATP) as a signal molecule also plays an indispensable role in regulating cellular metabolism and biochemical synthesis in living systems. Intracellular ATP abundance is high enough (ranging from 1 to 10 mM),[35] making ATP a potentially promising biomarker for amplification detection. Importantly, extracellular ATP in tumor tissues is usually more than 4 orders of magnitude higher than that in normal tissues, and thus tumor tissues can be well distinguished.[36]

Zhang's group invented an ATP-self-powered strand-displacement cascade amplification (SDCA) system of mesoporous silica nanoparticles modified by Y-motif DNA structures (CuS@mSiO2/Y-ATP) for the detection of low-abundance miRNAs in living cells. Upon cellular uptake, the folded DNA strand is unlocked by forming a C−G ·C+ triple DNA structure and accelerating the breakdown of disulfide bonds, which releases large amounts of ATP in the acidic tumor micro-

https://doi.org/10.1021/prechem.4c00100
Precis. Chem. 2025, 3, 187−205

environment (TME). Endogenous specific miRNAs initiate displacement of the corresponding strand, and ATP is used as fuel for SDCA to generate the corresponding fluorescence for miRNA target detection (Figure 3A).[37] Liang et al. developed an endogenous ATP-powered 3D DNA walker on the soft surface of DNA nanospheres, which could execute autonomous movement under the stimulation of overexpressed miR-21 in a TME for sensitive miR-21 detection and sensing in living cells. When a 3D walker enters a living cell, miR-21 binds to the blocking chain, releasing the walking chain and triggering an ATP-driven walking response. The 3D walkers' walking then produced an enhanced Cy3 fluorescence signal, indicating the amount of miR-21 (Figure 3B).[38] Meng et al. reported a novel target cell-specific DNA nanosystem that utilized the amplification of biologically orthogonal activated HCR signals from endogenous ATP to image miRNA-155 in living cells and in vivo. The HCR hairpin probe is blocked by ATP aptamers and loaded into a GSH-coated tumor cell membrane (CM)-responsive metal−organic framework (MOF) (MOF-h1/H2@CM) (Figure 1). After internalization, MOF nanoparticles rapidly degrade and release H1 and H2 in the presence of GSH. Endogenous ATP binds to aptamers, releasing H1 while activating HCR and amplifying miRNA signals (Figure 3C).[39]

Lei et al. designed an ATP-driven and accelerated fluorescent luminescent 3D DNA Walker (FLDW) biosensor for sensitive detection and imaging of miRNA-221 in tumor cells.[40] FLDW consists of AuNP carrying a hairpin probe H3, combined with a two-strand track (S/a) hybridized by a G-rich sequence chain (S) and an ATP-containing aptamer chain (a). In addition, two hairpin probes, H1 and H2, were triggered by miRNA-221 to amplify CHA. H2 has a Mn^{2+} dependent DNAzyme catalytic domain, cleaved substrate H1 in the presence of Mn^{2+}, produced a large number of output chains, and specifically unfolded the hairpin junction of H3. The released H3 binds to a, exposing the G-rich sequence in S to form a G4 structure, embedding ThT in G4, and emitting a partial fluorescence signal. ATP then spontaneously binds to A, releasing the free-swinging H3 to diffuse along the DNA-AuNP orbit and automatically capture another A strand from the adjacent S/A orbital. Finally, ThT was embedded in an increasing number of G4 pairs, and the rapid accumulation of a large number of fluorescence signals ultimately enabled sensitive and rapid labeling-free detection of the low abundance target miRNA-221.

GSH-Responsive NDARs. Glutathione (GSH) is the most abundant small molecule antioxidant in cells and plays a key role in cell growth and function. The concentration of GSH in cells has been reported to be about 2−10 mM as compared with around 2−40 μM in the extracellular fluid. More importantly, GSH in cancer cells is at least 4 times higher than that in most normal cells.[41] Based on the spatially distinctive concentrations of GSH, researchers have developed sensitive nanoplatforms to enhance the specificity of tumor diagnosis and tumor therapy. Despite most of the research applying a platform to carry DNA probes, which are reactive with GSH to release certain ions, we focus on only the scenarios where GSH reacts directly with DNA to induce the ensuing amplification reactions. Although this remains less explored so far, GSH-regulated amplification methods provide a knowledgeably reliable and effective means for accurate miRNA analysis and offer new insights into the underlying signaling pathways of miRNA regulation.

Chen et al. successfully designed a GSH-responsive DNAzyme-based nanodevice that maintains stability in blood vessels and can be activated by high concentrations of GSH after targeting and entering tumor cells. GSH broke the disulfide bond of the hairpin structure, miRNA hybridized with the exposed hairpin structure to further open the signal output element of DNAzyme, and in the presence of magnesium ions, the DNAzyme cut the substrate to release a fluorescent signal. The nanosensor had successfully realized the imaging analysis of miRNA-21 in subcutaneous tumors in mouse models (Figure 4A).[42] Wang et al. designed an HCR nanosensor that responds to GSH. The hairpin probe was sealed by the disulfide bond, GSH cut the disulfide bond to expose the foothold, and miRNA-21 was further bound to the hairpin probe to open the HCR and achieve fluorescence signal amplification.[43]

Light-Responsive NDARs. Light-activated nanomachines have high sensitivity and fewer false positive results. Many studies have included light-sensitive switches in nucleic acids or proteins to control light activation in time and space. Compared to traditional passive response methods, light-activated designs can provide highly accurate spatiotemporal control for sensing and imaging. So far, various light-activated designs have been reported for sensing and imaging intracellular miRNAs.[44−46]

Wang et al. developed a near-infrared orthogonally programmed DNA nanomachine with a light-locked DNAzyme for precise in vivo imaging of low-expressing miRNA in the early tumor stage. DNA nanomachines had realized cancer detection earlier than the size monitoring imaging technology and amplified the in vivo NIR-II imaging signal of early tumor miRNAs, which had a promising application in early cancer detection.[47] Hao et al. proposed a NIR-initiated Photoelectrochemical biosensor based on csUCNRs@TiO_2@CdS for miRNA-133a detection. MiRNA-133a and hairpin probes initiated magnetic-bead-assisted HCR, producing long-chain nucleic acid products that carried alkaline phosphatase. The HCR product catalyzed the formation of ascorbic acid (AA) from ascorbic acid 2-phosphate. AA consumed photoelectric holes on the surface of csUCNRs@TiO_2@CdS, with 980 nm light excitation to generate photocurrent. At the same time, the oxidation product of AA, dehydroascorbic acid, was reduced to AA by tri -(2-carboxyethyl) phosphine at the detection end for cyclic amplification to achieve more sensitive miRNA detection (Figure 4B).[48]

Multistimuli-Responsive NDARs. Multistimuli-responsive miRNA detection is an advanced method of molecular diagnosis, which uses multiple response molecules to control the activation of cell imaging and detection. In the complex disease microenvironment, the multistimuli-responsive can further improve the selectivity, sensitivity, and accuracy of detection. The combination of different stimuli reduces background noise and minimizes false positives, making it an important approach for early disease detection and treatment monitoring.

Ye et al. designed an intelligent NIR-light-activated 3D DNA walker powered by ATP for miRNA in situ detection. UCNPs acted as a DNA carrier and light conversion element, binding o-nitrobenzene (PC) groups. Under NIR irradiation, UCNPs released ultraviolet light to cut the PC group, released the hairpin probe, activated the DNA walker, and unlocked the walking chain. The DNA walker walking chain bound to the ATP aptamer chain carrying fluorophores, and when ATP bound to aptamer in the cell, the walking chain was released, so that it continued to bind to other aptamer chains, thus carrying out the cycle and continuously producing fluorescence (Figure 4C).[49] Wang's research group designed a tumor-specific protease-activated nanosensor system (PA-NS) for dual-model

https://doi.org/10.1021/prechem.4c00100
Precis. Chem. 2025, 3, 187−205

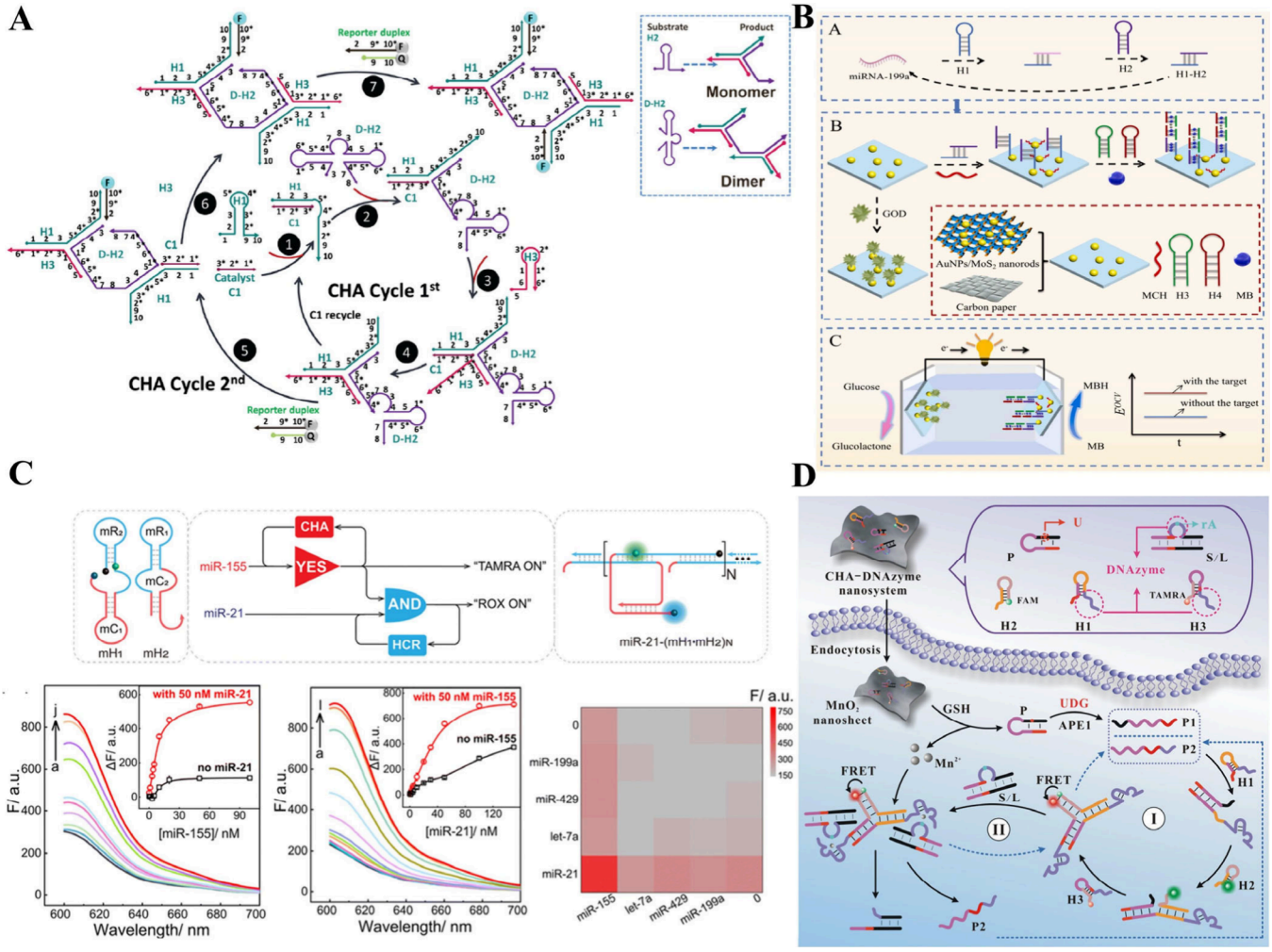

Figure 5. CHA-triggered cascade NDARs. (A) 3-way CHA-CHA cascade circuit. Reproduced with permission from ref 54. Copyright 2020 American Chemical Society. (B) Electrochemical/colorimetric dual-mode detector based on CHA-HCR. Reproduced with permission from ref 58. Copyright 2023 Elsevier. (C) CHA-HCR cascade circuit with double superhairpin for microRNA cell imaging. The method showed a sensitive detection performance and realized simultaneous detection of miR-21 and miR-155. Reproduced with permission under the terms CC BY from ref 59. Copyright 2023 Dong et al. (D) CHA-DNAzyme cascade circuit for UDG in situ detection and imaging. Reproduced with permission from ref 65. Copyright 2021 American Chemical Society.

sensing of miR-21 through coupled optical imaging and electrochemical detection.[50] The fluorescence chain and electrochemical reaction chain (BHQ-DNA) were hybridized and combined with the peptide nucleic acid−peptide−peptide−nucleic acid complex to form the detection system.

In tumor cells, PA-NS was selectively activated by overexpressed CaB proteases, and miR-21 underwent chain substitution, releasing BHQ-DNA, and generating the fluorescence signal. The released BHQ-DNA had a chain displacement reaction with the dsDNA-modified electrode, resulting in the desorption of $Ru(NH_3)_6Cl_3$ and the generation of an electrochemical signal.

Chen et al. designed a sequentially responsive aptamer sensor that uses the "and" logic gate to sensitively and accurately identify cancer cells. Aptasensor contained strands that responded to the acidic environment of cancer cells, an ATP aptamer, and an aptamer that anchored the target cell. The Y-shaped structure of the three-strand hybridization was anchored to the cell membrane, and the acid response structure changed to expose the ATP binding site and the ATP aptamer bound ATP to generate fluorescence signals. DNA logic devices were constructed using pH changes and extracellular ATP to avoid false negative signals. In addition, the precise computational power of the "and" logic gate can further improve the accuracy of tumor cell imaging (Figure 4D).[51] It is worth mentioning that tumor-specific multistimulus-responsive NDARs enhance the sensitivity and selectivity of miRNA in tumor cells and are expected to be applied in cancer diagnosis due to the programmable activation system.

Cascade NDARs

Single-layer NDARs use a single amplification reaction, usually lack sufficient detection sensitivity, and present difficulties detecting ultralow target amounts. Cascade NDARs coupling two or more different amplification methods amplifies the detection signal multifold, thus having a lower limit of detection. Furthermore, cascade NDARs systems are widely utilized in cell imaging, attributed to their stable and rich nucleic acid products and compatibility with fluorescent labeling.

The design of DNA sequences for cascade circuits in NDARs is more complex due to their multilayer structure. Upper layer NDAR must be successfully triggered to activate the subsequent layer. Therefore, it is necessary to ensure the stability of hairpin

https://doi.org/10.1021/prechem.4c00100
Precis. Chem. 2025, 3, 187−205

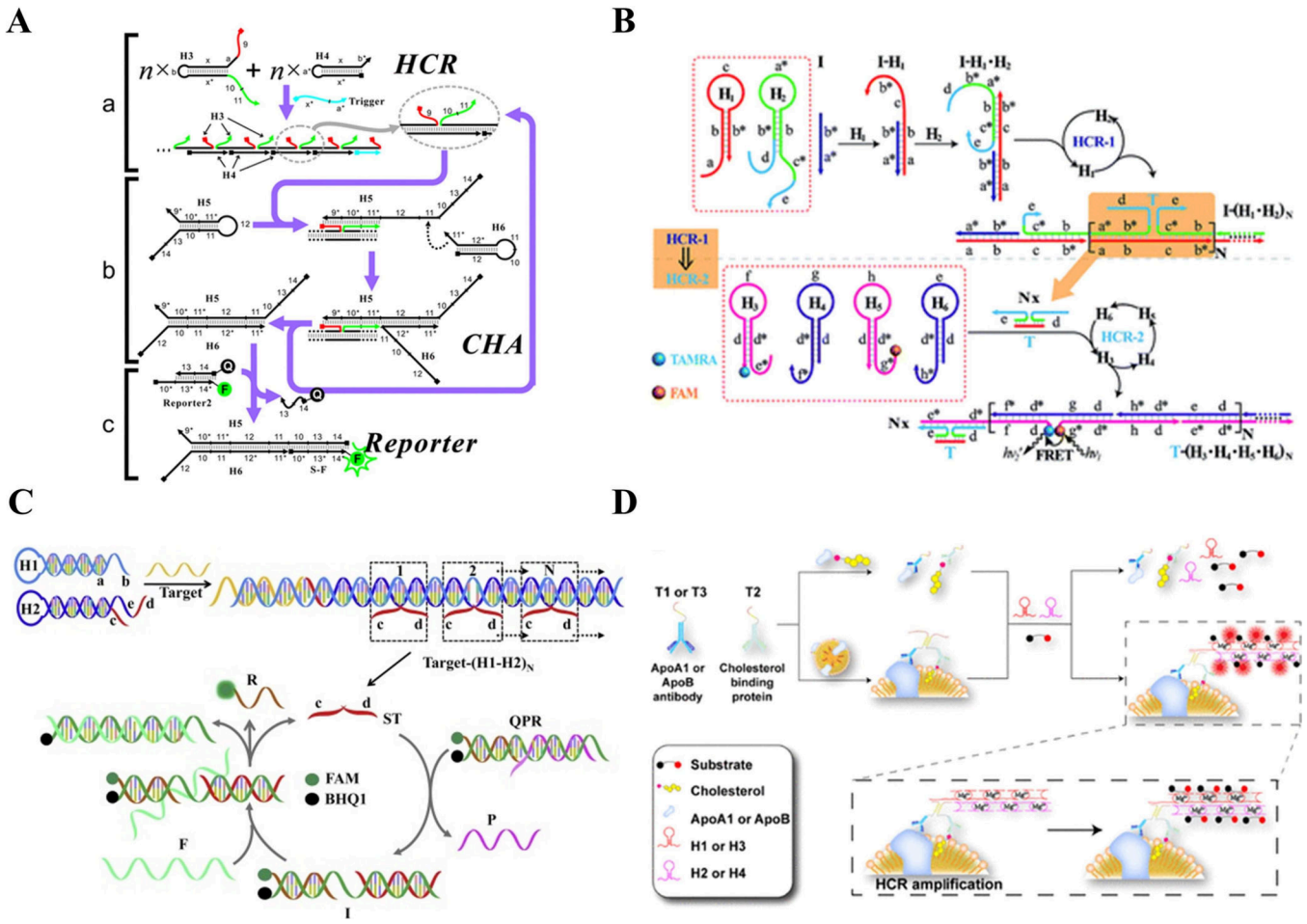

Figure 6. HCR-triggered cascade NDARs. (A) HCR-CHA cascade circuit. Reproduced with permission from ref 66. Copyright 2012 American Chemical Society. (B) HCR-HCR cascade circuit. Reproduced with permission under the terms CC BY from ref 67. Copyright 2018 Wei et al. (C) HCR-EDC cascade circuit. Reproduced with permission from ref 68. Copyright 2018 Elsevier. (D) HCR-DNAzyme cascade circuit for lipoprotein detection. Reproduced with permission from ref 69. Copyright 2021 American Chemical Society.

probes to prevent the spontaneous opening of downstream NDARs, which could cause signal leakage.[52] Typically, the hairpin probes in downstream NDARs are designed with greater thermodynamic stability. Additionally, the reaction dynamics of cascade NDARs must be carefully considered. The toehold sequences should be optimized to facilitate the reaction and prevent NDARs from reaching premature equilibrium, thereby enhancing the amplification efficiency of cascade NDARs.

Compared with single-layer NDARs, multilayer NDARs have more potential for accurate diagnosis. Different cascade NDARs are initiated by different amplification reactions, which can be divided into HCR/CHA/EDC/DNAzyme-triggered cascade circuits. Meanwhile, multilayer cascade NDARs have been developed by coupling multiple CHA, HCR, DNAzyme, and EDC, achieving ultrasensitive diagnosis.

CHA-Triggered Cascade NDARs. The first CHA-CHA NDARs were constructed by Chen et al., which used the stem structure of the first layer of CHA to block the toehold of the second layer of CHA, reducing the background signal caused by the catalyst, resulting in a 7000-fold amplification of fluorescence signal and a 10-fold increase in signal-to-noise ratio compared to the single CHA reaction.[53] The cascade reaction using multiarms-based CHA reduced the background signal. The development of 3way-CHA further reduces the risk of CHA circuit leakage and background signals. Zhu et al. tested the recognition ability of solid-state nanopores through 3way-CHA-CHA circuits. By introducing hairpin probe H2 containing two CHA reaction structures, H2 combined with two sets of hairpin structures to form a dimer. The dimer contains the fluorescence signals of two-layer CHA-CHA circuits, increasing the fluorescence signal intensity and improving the detection accuracy (Figure 5A).[54] CHA-HCR NDARs first use the catalyst to initiate the CHA reaction, producing CHA product carrying free terminal DNA strands that activate HCR amplification. The simultaneous operation of two cycles of HCR and CHA made the detector highly sensitive.[55] CHA-HCR achieved signal amplification of other biomarkers, such as proteins and bacteria, by combining aptamers. Zou et al. used aptamer to specifically capture *H. pylori* in feces, and unlocked CHA-HCR NDARs by releasing the catalytic chain bound to aptamer, achieving sensitive fluorescence detection.[56]

By combining different signal sensors, we could further improve the detection accuracy of CHA-HCR could be further improved. Song et al. used CHA-HCR for dengue virus DNA signal amplification and detected HCR reaction products using the SERS detection platform. The reaction sensitivity was 4.5 times higher than that of a single CHA.[57] Shi et al. used the colon cancer suppressor gene miRNA-199a as a catalyst to activate CHA-HCR, and the nucleic acid chain of HCR acted as the

https://doi.org/10.1021/prechem.4c00100
Precis. Chem. 2025, 3, 187−205

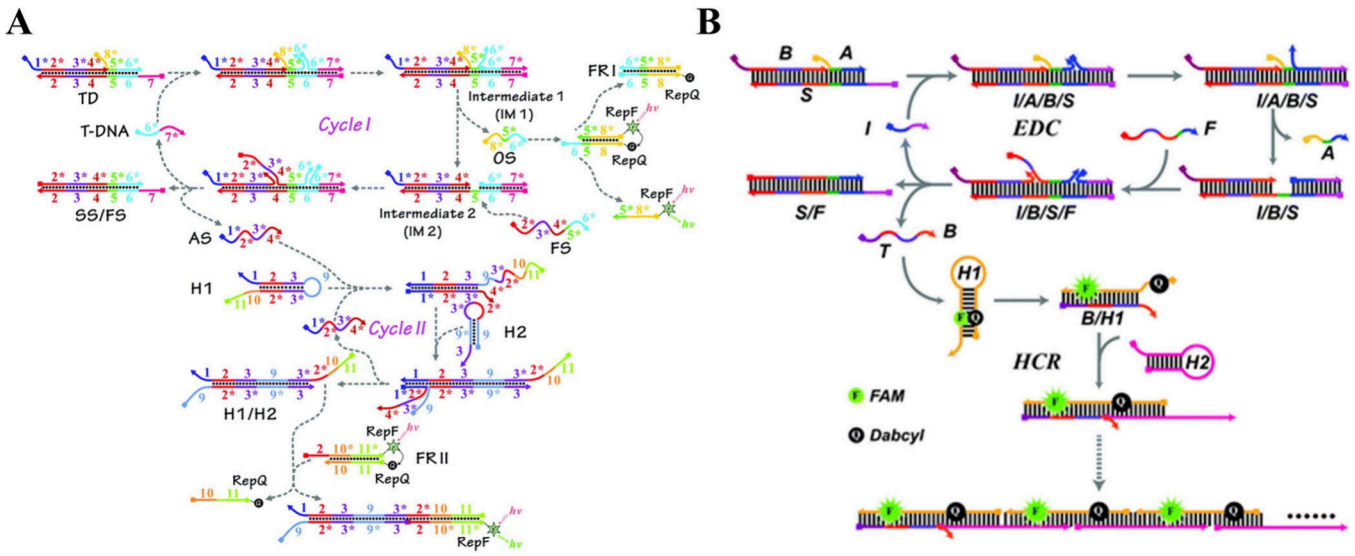

Figure 7. EDC-triggered cascade NDARs. (A) EDC-CHA cascade circuit. Reproduced with permission from ref 71. Copyright 2018 Royal Society of Chemistry. (B) EDC-HCR cascade circuit. Reproduced with permission from ref 72. Copyright 2020 Royal Society of Chemistry.

electrode cathode carrying a negative charge to attract methylene blue. The reduction reaction of methylene blue generated an open circuit voltage and caused a change in solution color, establishing a colorimetric/electrochemical detector (Figure 5B).[58]

CHA-HCR produced polylong nucleic acid chains, usually carrying fluorophores. They are widely used in cell imaging because of their stable and sensitive fluorescence signals in cells. Dong et al. designed two superhairpin structures that reduced the reaction substrates required for CHA-HCR. The input of two different microRNAs activated CHA and HCR to generate two kinds of fluorescence signals, which realized the simultaneous imaging of multiple microRNAs and more sensitive identification of cancer cells (Figure 5C).[59] Li et al. used pHCR with palindromic sequence to improve the aggregation degree of CHA-HCR products, so as to improve the imaging accuracy. After CHA was initiated by miRNA, CHA reaction products further initiated HCR with palindromic sequence, and the linear HCR products were cross-linked to each other to form a nucleic acid chain network and enhance the aggregation of fluorescent signals.[60] Chao et al. developed a dual-target CHA-HCR imaging system using nucleic acid strand displacement to control the opening and closing of the toeholds. The dual target probes bound microRNA-892b to expose the toeholds, which further bound microRNA-21 and hindered the initiation of CHA cycling. When the amount of microRNA-21 in cancer cells was greater than that of microRNA-892b, excess microRNA-21 participated in the CHA-HCR circuits and generated fluorescent signals. The dual-target imaging system further improved the accuracy of cancer cell imaging.[61]

In CHA-DNAzyme NDARs, Pan et al. designed hairpin probes containing aptamer sequences for binding mycotoxins and exposing the activation strand to turn on CHA. CHA products were used to assemble DNAzyme, and fluorescent probes were cleaved to obtain signals.[62] Improving the universality of NDAR detection could be achieved with different aptamer designs.[63] Shen et al. developed a 3D-DNA-walker based on CHA-DNAzyme for detecting telomerase activity. Telomerase and primer reactions allowed the primer to grow and initiate CHA, and the two hairpins assembled as DNAzyme to cleave the fluorescent reporter catalyzed by magnesium ions. The combination of 3D-walker and CHA-DNAzyme allowed a fast reaction rate and high sensitivity.[64] Song et al. developed a CHA-DNAzyme assay for Uracil DNA glycosylase (UDG) detection and cell imaging. MnO_2 was used as a nanocore to deliver DNA probes and degraded in the cell to produce Mn^{2+}, which occurred as a cofactor of DNAzyme. The 3way-CHA was turned on after UDG cutting the probes, and the CHA product as the cutting substrate of DNAzyme, obtaining the output chain to initiate the next round of CHA (Figure 5D).[65]

HCR-Triggered Cascade NDARs. In the HCR-triggered cascade reaction, HCR was usually designed to react with four hairpin structures, and the multihairpin design further reduced the background signal. In HCR-CHA NDARs, the catalyst of CHA was divided into two segments designed in the hairpin of HCR. The two terminal free DNA strands in the HCR reaction product formed a T-shaped structure and were used as the catalyst to start the CHA reaction (Figure 6A).[66]

The first layer of HCR-HCR contained two hairpin structures. The HCR product contained the T structure, which activated the second layer of HCR to form a long nucleic acid chain containing four hairpin structures. At the same time, only the initiation chain of the first layer of HCR needed to be designed to expand the detection range and apply to different targets, making HCR-HCR programmable (Figure 6B).[67] Zhang et al. used the HCR-HCR cascade circuit to analyze intracellular polynucleotide kinase (PNK) activity and performed in situ detection and imaging of PNK. The product of PNK cutting the hairpin probe activated HCR, and the long chain nucleic acid product of the first layer of HCR contained abundant terminal-free chains, forming T structures to open the next layer of HCR, and obtaining stable fluorescence signals.[70]

Similar to other HCR cascades, the HCR-EDC/DNAzyme NDARs are initiated by the HCR. HCR obtained a T structure containing two ends of the free DNA strand, which was used as a target to turn on the EDC, combined with a three-strand duplex. The addition of the fuel chain releases fluorescent reporters and HCR products for the next EDC cycle (Figure 6C).[68] Chen et al. developed HCR-DNAzyme cascade NDARs for lipoprotein detection. High-density lipoprotein (HDL) and low-density

https://doi.org/10.1021/prechem.4c00100
Precis. Chem. 2025, 3, 187−205

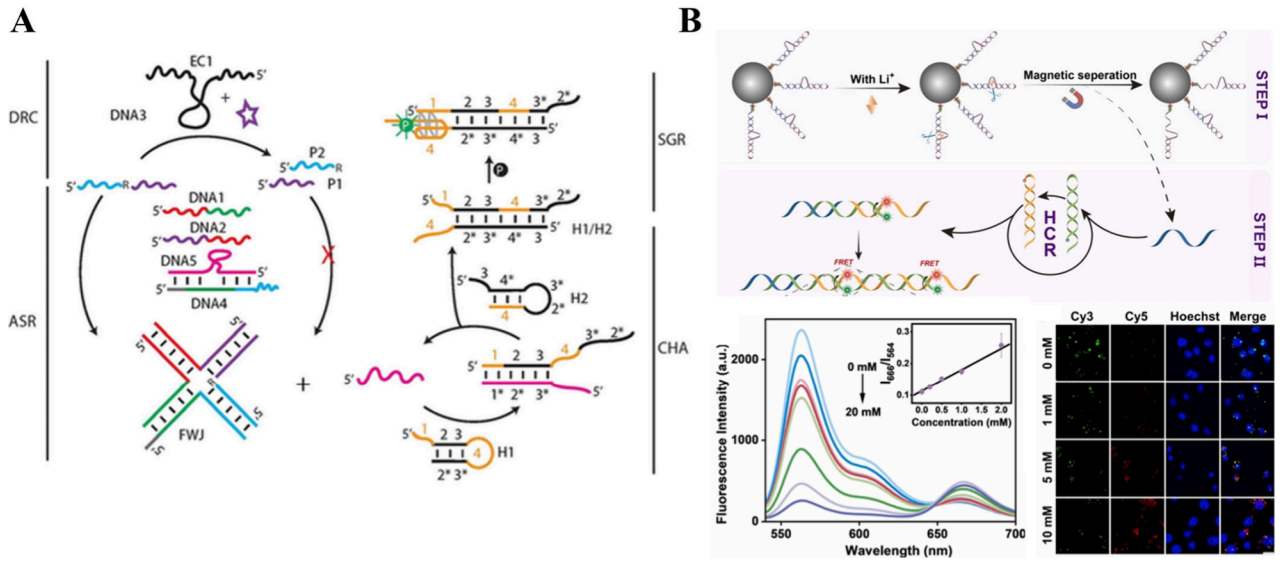

Figure 8. DNAzyme-triggered cascade NDARs. (A) DNAzyme-CHA cascade circuit of 4-way junction DNA for RNA detection. Reproduced with permission from ref 74. Copyright 2020 John Wiley and Sons. (B) Li^+-Based DNAzyme-HCR cell imaging method. The method demonstrated a sensitive detection performance and realized intracellular imaging. Reproduced with permission from ref 79. Copyright 2024 Elsevier.

lipoprotein (LDL) bound DNA single strands coupled with different antibodies, respectively, and each protein bound two DNA single strands to form hybrid double strands. The hybridization strand opened the hairpin structure and initiated the HCR. HCR products contained multiple DNAzyme structures that were used to cleave the fluorescence reporter, producing amplified signals (Figure 6D).[69]

EDC-Triggered Cascade NDARs. The cascade circuit opened by EDC has a higher stability and reduces the possibility of signal leakage. For the EDC-CHA NDARs, the target DNA binds to the double-stranded substrate to release the output chain, the output chain and the fluorescence reporter hybridize to obtain the fluorescence signal, and the fuel chain is added to release the target DNA, and the catalyst of CHA, thus opening the CHA. Fluorescence reporters were applied to both amplification reactions, which consumed the product and promoted the reaction cycle (Figure 7A).[71] In the EDC-HCR cascade circuit, the target strand generated by EDC initiation opens the hairpin of H1, thereby opening HCR and achieving signal amplification(Figure 7B).[72] Zhang et al. developed an EDC-driven dumbbell DNAzyme intracellular assembly and used it for uracil-DNA glycosylase (UDG) in situ detection and imaging. The UDG-cleavage substrate was used as a target to turn on the EDC, and the fuel chain was catalyzed to form a dumbbell EDC product containing two reaction sites for DNAzyme. Catalyzed by the cofactor Mg^{2+}, DNAzyme cleaved the fluorescence reporter to produce amplified signals. Full conversion of EDC products to DNAzyme reduced losses and further improved detection accuracy.[73]

DNAzyme-Triggered Cascade NDARs. DNAzyme had similar functions to enzymes in the cleavage of RNA/DNA substrates, higher stability, and its own nucleic acid structure, which made DNAzyme easier to combine with other NDARs. For DNAzyme-CHA NDARs, Zhou et al. used DNAzyme with RNA cleavage activity, and combined multiple DNA strands to build a 4-way junction DNA structure, constructing a signal converter for RNA signals. In the presence of the RNA target, DNAzyme cleared the substrate, impeded the formation of the 4-way junction, which prevented the release of the catalyst and inhibited CHA, thus linking the RNA input signals with the fluorescence signals (Figure 8A).[74] Zhou et al. developed an epigenetic analysis method of DNAzyme-CHA based on the different cleavage efficiencies of DNAzyme for different methylation targets. Targets with different methylation degrees led to different amounts of DNAzyme cleavage products, which affected the reaction time of cleavage products to CHA, so as to distinguish whether DNA was methylated according to different CHA reaction signals.[75] Huang et al. used DNAzyme-CHA for intracellular imaging of microRNA-21. The binding of microRNA-21 to the complementary strand released the input strand, activated DNAzyme, and cleaved the hairpin substrate. The cleaved substrate turned on the CHA to obtain amplified fluorescence signals.[76] Zhu et al. combined aptamer-based DNAzyme with 3-way CHA to develop non-nucleic acid target cascade NDARs for in situ detection and imaging of ATP. The combination of ATP and aptamer altered the conformation of DNAzyme, cleaving the hairpin substrate under Mg^{2+} catalysis and opening the 3-way CHA. The CHA products of the three hairpin substrates carried more fluorophores, resulting in more concentrated fluorescence signals, improving detection and imaging sensitivity.[77] Chen et al. developed an electrochemical assay based on DNAzyme-HCR for the detection of alpha-fetoprotein (AFP). AFP was captured by the sandwich-antibody method, which carried streptomycin and simultaneously coupled DNAzyme. Catalyzed by Cu^{2+}, DNAzyme cleaved the substrate and bound the hairpins to open the HCR. HCR products affect electrode electron transport and were therefore sensitively detected.[78] Wang et al. used the DNAzyme-HCR cascade circuit for the origin detection and imaging of intracellular Li^+. DNAzyme was activated under the catalysis of Li^+, and the cleaved substrate exposed the initial sequence of HCR, thus turning on HCR and quenching the fluorescence signal (Figure 8B).[79]

Multilayer Cascade NDARs. The multiple cascades of HCR, CHA, and DNAzyme further improved the signal amplification ability. Wang et al. introduced a catalyst into HCR-CHA NDARs to accelerate the reaction and designed an efficient cascade that required only three hairpins, and the target

https://doi.org/10.1021/prechem.4c00100
Precis. Chem. 2025, 3, 187−205

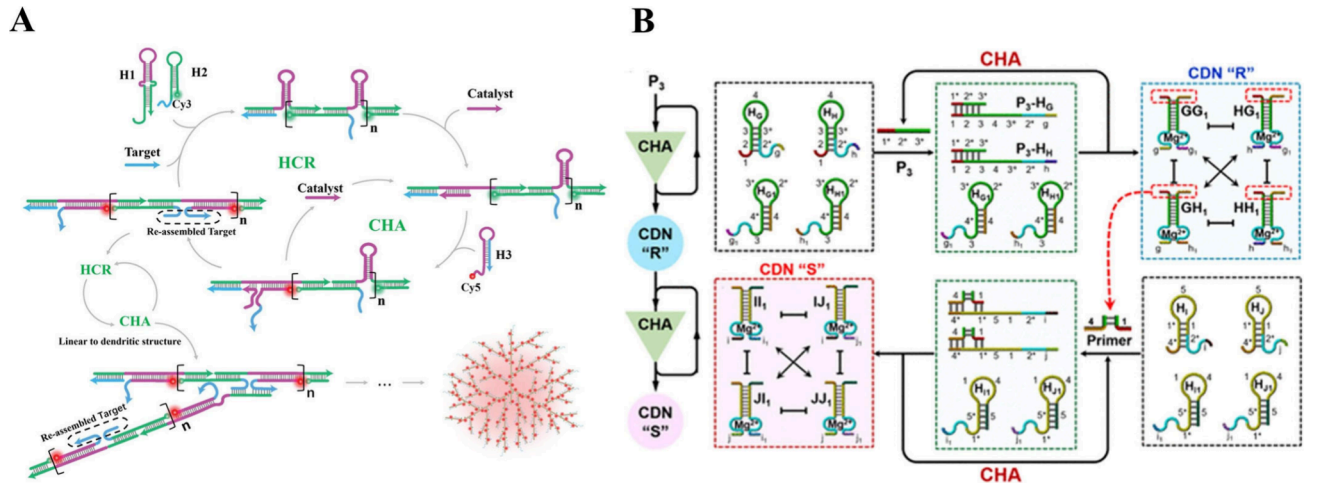

Figure 9. Multilayer cascade NDARs. (A) HCR-CHA-HCR multicascade circuit. Reproduced with permission from ref 80. Copyright 2023 John Wiley and Sons. (B) CHA-CDN (DNAzyme constitutional dynamic network)-CHA-CDN multicascade circuit. Reproduced with permission from ref 81. Copyright 2023 American Chemical Society.

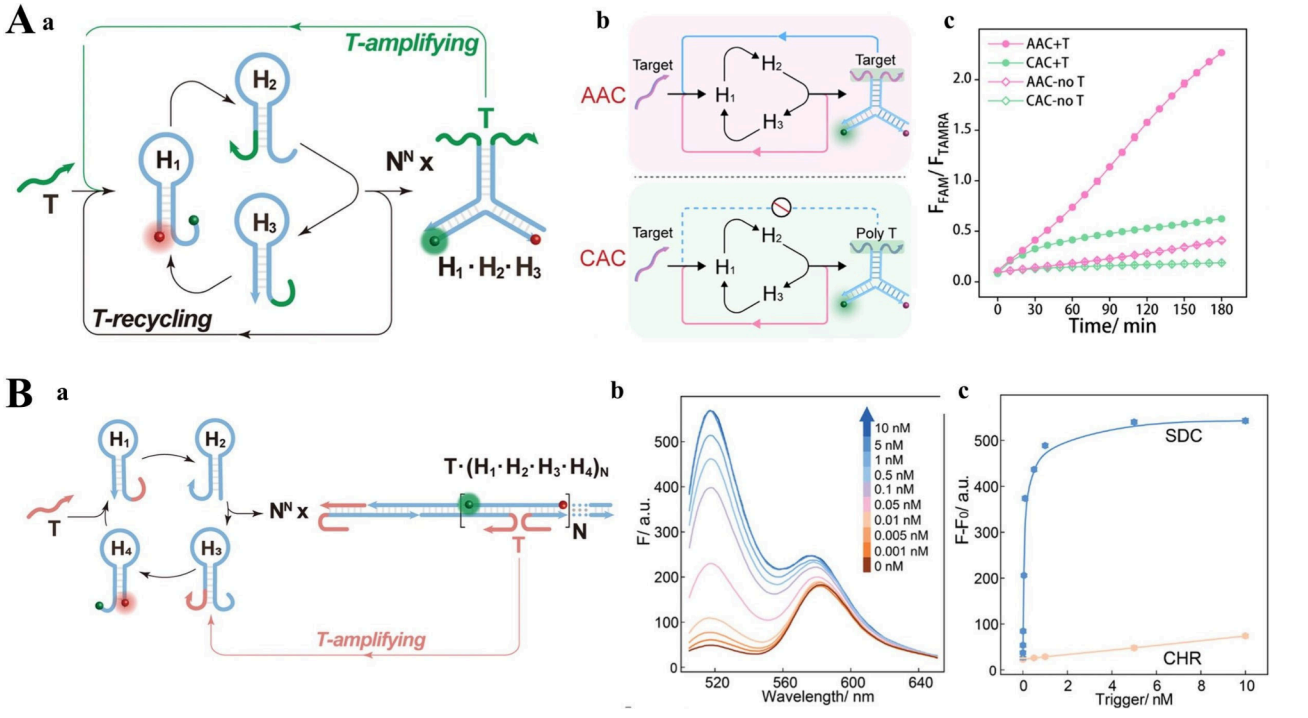

Figure 10. Scheme of single-layered autocatalytic NDARs. (A): (a) CHA-based single-layer autocatalytic NDARs. (b) Logic diagram shows the differences between the autocatalytic and the nonautocatalytic systems. (c) Time-dependent fluorescence ratio changes of the AAC system and CAC system in the absence and presence of target T (5 nM). Reproduced with permission from ref 92. Copyright 2023, American Chemical Society. (B): (a) HCR-based single-layer autocatalytic NDARs. (b) Fluorescence spectra of the HCR-based autocatalytic circuit (SDC) upon the addition of T with varied concentrations. (c) Comparison of the SDC and CHR (cascade hybridization reaction, similar to HCR) systems upon the determination of T with different concentrations. Reproduced with permission from ref 93. Copyright 2023, John Wiley and Sons.

initiated the HCR and partially opened the hairpin 1. The addition of catalyst opened hairpin 1 and reacted with hairpin 3 to initiate the CHA reaction, forming long nucleic acid chain products containing three hairpins. The free ends of hairpin 2 and 3 formed T structures, initiating branched chain HCR amplification, and finally forming a multifold cascade HCR-CHA-HCR method (Figure 9A).[80] Zhou et al. reported a cascade signal amplification technique for bilayer CHA combined with DNAzyme. The catalyst initiated the binding of the four hairpin structures in pairs and bound magnesium ions to form DNAzyme while activating the next layer of CHA to trigger the binding of the hairpin to form another DNAzyme. Both DNAzyme cleaved the fluorescent reporter simultaneously to show the progression of CHA and avoid false positive signals (Figure 9B).[81] Liu et al. used DNAzyme coupled HCR and CHA for the detection of *E. coli*. In the absence of *E. coli*, DNAzyme was inactivated for cleaving the substrate, which in turn activated HCR-CHA cascade amplification and caused changes in the fluorescence signals.[82] Wang et al. constructed a CHA-DNAzyme-HCR reaction system for miRNA detection.

https://doi.org/10.1021/prechem.4c00100
Precis. Chem. 2025, 3, 187−205

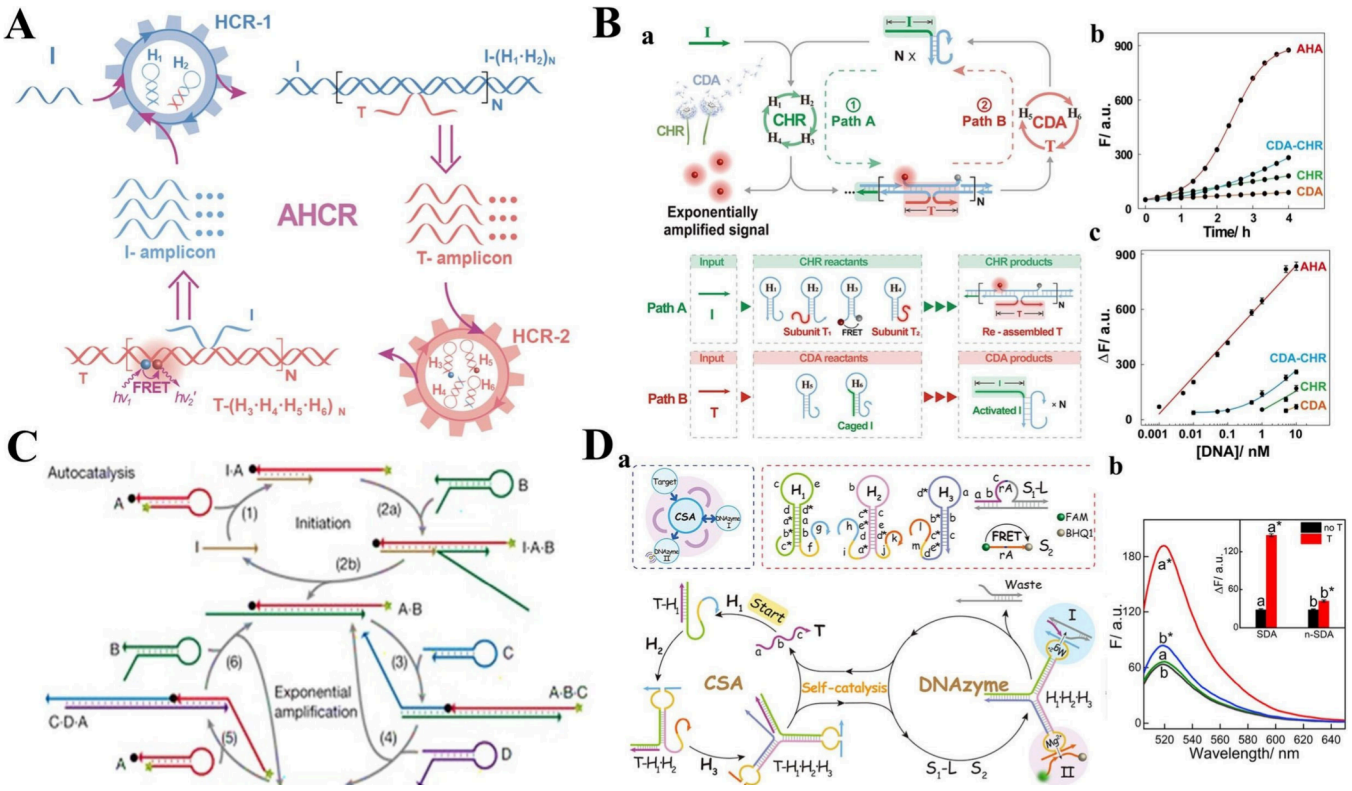

Figure 11. Scheme of two-layered autocatalytic NDARs. (A) HCR-HCR cross-catalyzed circuit. Reproduced with permission from ref 94. Copyright 2023, Chinese Chemical Society. (B): (a) HCR-CHA cross-catalyzed circuit. (b) Time-dependent fluorescence of cross-catalyzed HCR-CHA(AHA), cascade HCR-CHA(CDA-CHR), HCR(CHR), and CHA(CDA) upon analyzing their respective targets. (c) The corresponding calibration curve of these systems. Reproduced with permission from ref 95. Copyright 2022, John Wiley and Sons. (C) CHA-CHA cross-catalyzed circuit. Reproduced with permission from ref 97. Copyright 2008, Springer Nature. (D): (a) CHA-DNAzyme cross-catalyzed circuit. (b) Fluorescence spectra generated by the cross-catalyzed circuit (SDA) and nonautocatalytic circuit (n-SDA) sensing systems in the absence and presence of target T (10 nM). (c) Fluorescence intensity changes (λ = 520 nm) of the SDA and n-SDA sensing systems. Reproduced with permission from ref 96. Copyright 2008, American Chemical Society.

miRNA221 was triggered as a target to activate CHA, while the two hairpin structures combined as a DNAzyme to cleave the substrate and release the output strands. The output strands opened the hairpins fixed on the electrodes and initiated HCR, resulting in an ultrasensitive, high signal-to-noise ratio electrochemical detection method.[83]

Autocatalytic NDARs

Compared to linear or cascade NDARs, autocatalytic circuits exhibit the highest signal amplification capacity due to their exponential growth characteristics.[21] NDARs that utilize toehold-mediated strand displacement (TMSD) offer a broad design space for creating autocatalytic systems, making them a promising approach for designing catalytic DNA circuits. In recent years, many NDARs, including CHA and HCR, have been used to construct autocatalytic DNA circuits by activating the self-assembly of reconfigurable DNA structures.[84−91] These autocatalytic NDARs can be broadly divided into two categories: single-layered autocatalytic NDARs and two-layered autocatalytic NDARs. Single-layered autocatalytic NDARs rely on a single circuit, where the product acts as the catalyst for its own formation. In contrast, two-layered autocatalytic NDARs involve two hierarchical circuits, with the products of each circuit cross-catalyzing the other's formation. While both approaches involve hierarchical reactions, they differ from cascade NDARs, where only the upstream circuit catalyzes the downstream circuit. This distinction gives autocatalytic NDARs unique amplification styles, with most exhibiting exponential amplification. However, it is important to note that exponential amplification of autocatalytic NDARs depends on maintaining an extremely slow background reaction. This minimizes unwanted signal leakage and ensures a high sensitivity. Despite their exponential nature, the supply of substrates is finite, leading autocatalytic NDARs to exhibit a sigmoidal kinetic profile: the reaction starts slowly due to the limited availability of catalysts, accelerates as the amount of catalyst increases, and ultimately slows down as the substrates are depleted. Below, we explore single-layered and two-layered autocatalytic NDARs in detail, along with their diagnostic applications.

Single-Layered Autocatalytic NDARs. Single-layered autocatalytic NDARs, as the name implies, are based on one simple circuit, which simplifies the design and greatly minimizes the undesired leakage associated with multilayered reactions. Single-layered autocatalytic NDARs currently have the simplest design, use the fewest DNA reactants, and exhibit exponential growth. Li et al. proposed a single-layered autocatalytic circuit with only one CHA circuit.[92] CHA could be activated upon recognition of analytes to form free analytes and Y-shaped DNA (H1·H2·H3), as shown in Figure 10A.

The target strand (T) was split into two segments that were, respectively, grafted and integrated into H2 and H3. The free analyte continuously activated CHA. Meanwhile, Y-shaped H1·H2·H3 reassembled the split target DNA sequence, activating CHA again. So, in the whole reaction, each cycle formed the

https://doi.org/10.1021/prechem.4c00100
Precis. Chem. 2025, 3, 187−205

product Y-shaped DNA with a reassembled target sequence that acts as the autocatalyst and recycled T to accelerate NDARs.

Theoretical simulations and experimental studies of this system revealed a sigmoidal kinetic profile, consistent with the characteristics of autocatalytic NDARs. The detection limit of the autocatalytic circuit toward the target DNA was 0.3 pM. By contrast, the detection limit of the traditional nonautocatalytic CHA system was acquired as 0.16 nM, which was 533-fold higher than that of the autocatalytic system. With the help of the auxiliary hairpin, autocatalytic NDARs were applied to detect microRNA-21 (miR-21). The detection limit was 1.7 pM and exhibited superior specificity among the parallel miRNAs. Additionally, the system was used for in vivo imaging of miR-21, where it produced a 2.1-fold fluorescence enhancement in tumor tissues compared to nonautocatalytic NDAR-treated controls.

HCR was also used for the construction of single-layer autocatalytic NDARs. Li et al. constructed single-layered autocatalytic NDARs based on HCR.[93] Four HCR hairpins were grafted with one split HCR trigger sequence: H1, H2, H3, and H4 (Figure 10B). Upon the presence of the target strand (T), the successive cross-opening of these hairpins was stimulated to yield linear dsDNA copolymers, where the split T segments were reassembled to generate new T sequences for continuously motivating the HCR circuit. This led to the autocatalytic reproduction of T, thereby accelerating the autocatalysis of HCR with exponential growth kinetics. The obtained detection limit of the autocatalytic circuit toward the target DNA was 0.6 pM, which is almost 670 times lower than that of traditional HCR amplifiers with linear-amplified capability. With the help of the H5, this HCR-based system was applied to detect miR-21 with a detection limit of 0.6 pM, exhibiting excellent selectivity and stability in complex biological samples. Encapsulation of this system in folic acid-modified nanoparticles enabled its use in in vivo imaging, yielding strong fluorescence signals in tumor-bearing mice. Notably, negligible fluorescence was observed in inhibitor-pretreated mice, demonstrating precise tumor-targeted miR-21 localization.

Two-Layered Autocatalytic NDARs. Two-layered autocatalytic circuits involve two hierarchical systems, in which the products of the upper and lower circuits catalyze each other. These circuits offer greater amplification capabilities compared to cascade circuits, where only the upper circuit catalyzes the downstream circuit. Two-layered autocatalytic NDARs are typically constructed by combining four linear amplification mechanisms (e.g., HCR, CHA, EDC, or DNAzyme) into cross-catalyzed systems. The upstream circuit's product acts as the initiator for the downstream circuit, while the downstream circuit's product catalyzes the upstream circuit, creating a feedback loop.

The HCR cross-catalyzed circuits represent the most diverse and versatile self-catalytic systems to date, encompassing HCR-HCR, HCR-CHA, and HCR-DNAzyme cross-catalyzed circuits.[87−91] The fundamental process begins with the activation of the target DNA strand, which initiates the HCR reaction and results in the formation of long dsDNA strands. Each repeating unit of the dsDNA monomer includes a recombinant trigger DNA sequence overhang that can initiate the downstream circuit. The product of this downstream circuit can then catalyze the upstream HCR reaction, creating an autocatalytic circuit. In a study by Zhang et al., a HCR-HCR cross-catalyzed system was developed for intracellular miRNA imaging. (Figure 11A).[94] The analytes initiated the activation of the first-layer HCR probes, resulting in the formation of long dsDNA strands that contained numerous intact initiators. These intact initiators subsequently triggered the second-layer HCR generating recombinant T, which in turn cross-catalyzed the first-layer HCR. Finally, the hyperbranched DNA assembly was produced and achieved exponential signal amplification. The system achieved a detection limit of 0.1 pM for miR-21 in vitro and provided robust Förster resonance energy transfer (FRET) signals in living cells, effectively distinguishing miR-21 expression levels in different cell types.

Despite the enhanced collision kinetics facilitated by the hyperbranched assembly of the two-layered HCR circuitry, the hyperbranched DNA products can cause steric hindrance, which may impair the reaction efficiency. Therefore, HCR-CHA and HCR-DNAzyme cross-catalyzed systems were developed to moderate the effects of steric hindrance.[91,95] Wang et al. introduced an HCR-CHA cross-catalyzed circuit, where the autocatalytic process began with the HCR circuit (Figure 11B).[95] Here, initiator I induced the autonomous cross-opening of HCR reactants, resulting in the formation of dsDNA nanowires. Concurrently, the subunits of T were brought together to form recombinant T, which served as a new trigger for the CHA circuit. These reconstituted triggers then initiated the CHA circuit, producing initiator I to cross-catalyze the upstream HCR circuit. The HCR-CHA cross-catalyzed system detected miR-21 with a detection limit of 0.5 pM in vitro. In living cells, it provided high specificity and robust fluorescence signals, distinguishing different miR-21 expression levels. In vivo, the system demonstrated high efficiency and specificity for miR-21 imaging in tumor-bearing mice with significant fluorescence observed at the tumor site.

CHA-CHA, CHA-HCR, and CHA-DNAzyme cross-catalyzed NDARs based on CHA- cross-catalyzed circuits have been reported.[88,96,97] The characteristic of these circuits is that the upstream CHA products are individual DNA double strands. Compared with the long dsDNA of HCR, the steric hindrance between DNA molecules is smaller, allowing for more flexible molecular movement. Target activation initiates the CHA reaction to form DNA double strands, which contain a trigger DNA sequence or recombine the trigger DNA strand of the lower circuit at the tail end, initiating the downstream circuit. The product of the downstream circuit then catalyzes the upstream CHA reaction, allowing the reaction to continue until the reactants are depleted. The first CHA-CHA cross-catalyzed NDARs were constructed by Yin et al.[97] The original T activated the upper CHA to catalyze the assembly of $H_A{\cdot}H_B$, and then $H_A{\cdot}H_B$ triggered the lower CHA forming $H_C{\cdot}H_D$, which contained a single-stranded overhang that was identical with the original T and could thus in turn cross catalyze the upper CHA to generate an exponentially amplified signal (Figure 11C). Wan et al. introduced a CHA-DNAzyme circuit consisting of multiple DNAzyme subunit-encoded CHA reactants and the substrates of DNAzyme.[96] As shown in Figure 11D, upon the presence of the analyte, the catalytic hybridization of CHA reactants initiated the formation of a Y-shaped DNA structure incorporating two distinct DNAzyme modules, I and II. DNAzyme module I catalyzed the production of new CHA initiators and catalyzed the CHA process. Meanwhile, DNAzyme module II functioned as a signal transducer, generating an FRET signal. The CHA-DNAzyme circuit sensing system detected miR-21 with a detection limit of 0.3 pM in vitro. In living cells, it provided robust fluorescence signals, accurately distinguishing the different miR-21 expression levels.

https://doi.org/10.1021/prechem.4c00100
Precis. Chem. 2025, 3, 187−205

EDC-based cross-catalyzed circuits have also proven to be effective for improving NDAR sensitivity. Xing et al. developed an EDC-DNAzyme circuit involving a three-strand duplex elongated with a silenced Mn^{2+} DNAzyme, a fuel strand, and an arched DNAzyme substrate hybrid (S/L duplex) containing one appropriately caged EDC initiator in the hybrid region.[86] In the presence of miR-21, miR-21 could circularly trigger the toehold exchange and branch migration reactions between the three-stranded duplex and F to generate a stable double-stranded complex with active Mn^{2+} DNAzyme, generating fluorescence signals. Simultaneously, with the coexistence of cofactor Mn^{2+}, after the target sequence initiated the EDC circuit, the active DNAzyme hybridized with the substrate sequence (S/L) and cleaved the ribonucleic acid site in S, leading to the *in situ* release of a new initiator analogue for the reverse feedback EDC reaction. This system achieved a detection limit of 21 pM for miR-21 and provided reliable imaging in living cells, demonstrating high biostability and biocompatibility.

CHALLENGE OF NDARS

Background Signal and Leakage

One of the most persistent challenges in NDAR systems, particularly in CHA and HCR, is the unintended signal leakage caused by the spontaneous opening of hairpin structures. These structures, essential for target-induced reactions, are designed with toehold regions to facilitate strand displacement. However, the metastable nature of hairpins allows them to occasionally open spontaneously due to thermal fluctuations, exposing reactive sequences prematurely and leading to undesired background noise and signal leakage. Moreover, thermal fluctuations, unintended cross-hybridization among hairpins, or nonspecific interactions within complex samples can destabilize the hairpin structures, leading to their premature opening. Besides, residual triggers, weak stem stability, and low energy barriers in designed sequences can also increase the chances of severe signal leakage. Consequently, this results in nontarget-initiated amplification and background signal generation, which significantly diminishes the signal-to-noise ratio. Meticulously designing thermally stable hairpins and applying blocking oligonucleotides to mask unintended binding sites or stabilize inactive states until the trigger is added can be expected to be conducive to minimizing leakage.

Probe Design and Optimization

The design of efficient and stable probes is critical to the success of NDAR systems. Probes must not only be specific to the target analytes but also exhibit high stability to prevent unintended interactions that could trigger false positives. However, the optimization of probes is a technically challenging task. A poorly designed probe may either fail to initiate the desired amplification or react prematurely, resulting in reduced specificity and sensitivity and thus remaining elusive due to the diversity of targets and the complexity of biological samples.

Reaction Efficiency in Complex Environments

NDARs demonstrate significant promise in controlled laboratory conditions, but their efficacy often diminishes in complex physiological environments such as the tumor microenvironment or body fluids. Factors such as high ionic strength, variable pH levels, and the presence of competing biomolecules can interfere with the amplification reactions, reducing their sensitivity and specificity. Additionally, the molecular crowding effect *in vivo* may impede the mobility and hybridization efficiency of nucleic acid probes.

Translation to Clinical Settings

Although NDARs have shown considerable promise in proof-of-concept studies, their translation to clinical diagnostics faces multiple hurdles. Scalability and reproducibility are critical challenges. NDAR systems often require synthetic DNA or RNA hairpins, probes, or triggers with high purity; hence, scaling the production of such oligonucleotides while maintaining quality can be indeed costly and time-intensive. Furthermore, in large-scale synthesis, slight deviations in oligonucleotide quality or purity can impact system performance, leading to inconsistent results, thus impeding its reproducibility. Worse still, NDAR systems often depend on fluorescence as produced by the nucleic acids that are prone to degradation over time; therefore, ensuring long-term stability under clinical storage conditions is a significant hurdle in clinical translation. Besides technical restraints, the regulatory approval process for clinical applications requires comprehensive validation of NDAR systems to ensure their safety, reliability, and efficacy. This includes demonstrating their performance in large-scale trials and addressing practical concerns, such as reagent stability.

Autocatalytic Circuit Stability

Autocatalytic NDARs, while offering unparalleled amplification potential, are prone to signal saturation, product accumulation, and instability during extended reactions. These issues arise from the exponential nature of autocatalysis, where the rapid generation of reaction products can deplete reagents, hinder subsequent amplification cycles, and lead to signal plateauing. Moreover, autocatalytic systems are particularly sensitive to minor perturbations under reaction conditions, which can amplify errors and reduce system reliability.

PROSPECT FOR NDARS

Enhanced Diagnostic Applications

NDARs have emerged as a powerful tool for biomarker detection, providing unparalleled sensitivity and cost-effectiveness. Unlike enzymatic systems, NDARs operate under relatively simple conditions, reducing the dependency on expensive enzymes and stringent protocols. This simplicity facilitates the early and precise diagnosis of diseases such as cancer, where the detection of low-abundance biomarkers is critical. Moreover, the programmability of NDARs allows them to target a wide range of analytes, including nucleic acids, proteins, and small molecules.[67] This versatility allows NDARs to be adaptable to diverse diagnostic applications. By enabling real-time detection and quantification, NDARs significantly improve disease monitoring, prognosis, and personalized treatment planning.

Integration with Advanced Technologies

The integration of NDARs with cutting-edge nanotechnology has unlocked new possibilities for bioimaging and therapy. For instance, the coupling of NDARs with gold nanoparticles, metal−organic frameworks (MOFs), and quantum dots has enabled the design of hybrid systems with enhanced signal transduction and amplification.[34,98,99] These nanomaterials not only improve the sensitivity of NDAR-based assays but also allow for multiplexed detection, where multiple targets can be identified simultaneously. Additionally, the incorporation of stimuli-responsive designs, such as pH-sensitive probes or ATP-triggered circuits, allows NDAR systems to function in complex biological environments.[30,37] This capability is particularly

https://doi.org/10.1021/prechem.4c00100
Precis. Chem. 2025, 3, 187−205

advantageous for real-time *in vivo* imaging, where external triggers such as light or magnetic fields can be used to control the reaction dynamics.[42,49] Such integrations position NDARs as cornerstones of technology for advanced diagnostics and therapeutic monitoring.

Point-of-Care Testing (POCT)

One of the most promising applications of NDARs is in point-of-care testing (POCT).[100] Unlike traditional nucleic acid amplification methods, NDARs eliminate the need for complex enzymatic reactions and highly controlled laboratory environments. This simplicity makes NDARs particularly suitable for resource-limited settings such as rural healthcare facilities or field-based diagnostics. Their portability and ease of use enable decentralized diagnostics, allowing patients to receive rapid and accurate results without the need for centralized laboratories. Furthermore, the low cost of NDAR reagents and devices enhances accessibility, bridging the gap between advanced diagnostics and underserved populations.

Synergy with Multistimuli Systems

NDARs demonstrate significant potential when combined with multistimuli-responsive mechanisms, which enhance their specificity and reduce false positives. Multistimuli systems rely on the simultaneous or sequential activation of NDARs by multiple environmental triggers, such as pH changes, light, or intracellular ATP levels.[51] This approach is particularly beneficial for applications in complex disease microenvironments, such as tumors, where multiple biochemical and physical factors coexist. By leveraging these factors, NDARs can achieve higher levels of specificity and selectivity, minimizing off-target effects. Such synergistic designs improve the reliability of NDAR-based assays, paving the way for their adoption in precision medicine.

Therapeutic Potential

Beyond diagnostics, NDARs exhibit immense therapeutic potential, particularly in the field of cancer treatment. NDAR-based systems, such as autocatalytic circuits and DNAzyme-powered frameworks, provide high signal amplification and programmable self-sustaining features. These characteristics make NDARs suitable for applications in drug delivery and therapeutic monitoring. For example, NDARs can be engineered to release therapeutic agents in response to specific intracellular conditions, such as elevated ROS or reduced pH, which are hallmarks of tumor microenvironments.[101] Additionally, the integration of NDARs with nanocarriers enables the targeted delivery of drugs to diseased tissues, reducing systemic toxicity and improving therapeutic efficacy.[102] Autocatalytic NDARs, in particular, hold promise for amplifying therapeutic signals in a self-reinforcing manner, ensuring sustained drug release and enhanced treatment outcomes. This dual role of NDARs in diagnosis and therapy underscores their potential as a transformative technology in the fight against complex diseases.

CONCLUSIONS

NDARs are revolutionizing nonenzymatic signal amplification by achieving exponential growth and enabling highly sensitive detection of biomarkers. NDARs stand at the forefront of innovative diagnostic and therapeutic solutions, representing a breakthrough in the field of nucleic-acid-based technologies and offering unparalleled versatility, sensitivity, and adaptability. Their puissant ability to integrate with multipotent nanotechnology, operate under diverse conditions, and synergize with multistimuli systems positions them as a cornerstone for future advancements in diagnostics and therapy. While challenges remain, ongoing advancements in circuit design and reaction optimization are paving the way for their integration into clinical diagnostics and therapeutic platforms.

AUTHOR INFORMATION

Corresponding Author

Hung-Wing Li − *Department of Chemistry, Faculty of Science, The Chinese University of Hong Kong, Hong Kong 999077, China*; orcid.org/0000-0003-4840-1965; Email: hungwingli@cuhk.edu.hk

Authors

Junyou Li − *Department of Chemistry, Faculty of Science, The Chinese University of Hong Kong, Hong Kong 999077, China*

Ting Li − *Department of Chemistry, Faculty of Science, The Chinese University of Hong Kong, Hong Kong 999077, China*

Zheng Zou − *Department of Chemistry, Faculty of Science, The Chinese University of Hong Kong, Hong Kong 999077, China*

Complete contact information is available at: https://pubs.acs.org/10.1021/prechem.4c00100

Author Contributions

#Junyou Li, Ting Li, and Zheng Zou contributed to this work equally.

Notes

The authors declare no competing financial interest.

ACKNOWLEDGMENTS

We are thankful for the financial support of the Hong Kong Research Grant Council (14300822) and the Chinese University of Hong Kong (CUHK). The TOC figure was created with BioRender.com. We are grateful to the original authors of the images used in the review.

VOCABULARY

Nonenzymatic DNA amplification reaction: A chemical process that amplifies DNA sequences without the use of enzymes, relying on the inherent properties of DNA and external stimuli to achieve signal amplification.

Biomarker detection: The identification and measurement of biological markers in samples, which can indicate the presence or progression of a disease.

Stimuli-responsive: Describes systems or materials that respond to specific external stimuli, such as changes in temperature, pH, or the presence of certain molecules, to trigger a desired action or response.

Cascade: A series of reactions or processes that occur sequentially, where the output of one step serves as the input for the next, often used to amplify signals in biological or chemical systems.

Autocatalytic: A reaction or process that is self-sustaining and self-amplifying, where the products of the reaction act as catalysts to promote further reactions, leading to exponential growth in signal or product formation.

Enhanced sensitivity: The improvement in the ability of a detection method to identify and quantify low levels of a target analyte, often achieved through signal amplification techniques like nonenzymatic DNA amplification.

■ ABBREVIATIONS

NDARs	Nonenzymatic DNA amplification reactions
NAs	Nucleic acids
TMSD	Toehold-mediated strand displacement
CHA	Catalytic hairpin assembly
HCR	Hybridization chain reaction
EDC	Entropy-driven circuits
ATP	Adenosine triphosphate
GSH	Glutathione
NIR	Near-infrared spectroscopy
miRNA	microRNA

■ REFERENCES

(1) Han, X.; Zhou, Z.; Fei, L.; Sun, H.; Wang, R.; Chen, Y.; Chen, H.; Wang, J.; Tang, H.; Ge, W.; Zhou, Y.; Ye, F.; Jiang, M.; Wu, J.; Xiao, Y.; Jia, X.; Zhang, T.; Ma, X.; Zhang, Q.; Bai, X.; Lai, S.; Yu, C.; Zhu, L.; Lin, R.; Gao, Y.; Wang, M.; Wu, Y.; Zhang, J.; Zhan, R.; Zhu, S.; Hu, H.; Wang, C.; Chen, M.; Huang, H.; Liang, T.; Chen, J.; Wang, W.; Zhang, D.; Guo, G. Construction of a Human Cell Landscape at Single-Cell Level. *Nature* **2020**, *581* (7808), 303−309.

(2) DeBerardinis, R. J.; Keshari, K. R. Metabolic Analysis as a Driver for Discovery, Diagnosis, and Therapy. *Cell* **2022**, *185* (15), 2678−2689.

(3) He, L.; Mu, J.; Gang, O.; Chen, X. Rationally Programming Nanomaterials with DNA for Biomedical Applications. *Advanced Science* **2021**, *8* (8), No. 2003775.

(4) Ang, Y. S.; Yung, L. Y. L. Protein-to-DNA Converter with High Signal Gain. *ACS Nano* **2024**, *18* (15), 10454−10463.

(5) Si, Q.; Li, Y.; Huang, Z.; Liu, C.; Jiao, T.; Chen, Q.; Chen, X.; Chen, Q.; Wei, J. Isothermal Reciprocal Catalytic DNA Circuit for Sensitive Analysis of Kanamycin. *J. Agric. Food Chem.* **2024**, *72* (12), 6754−6761.

(6) Zhou, Y.; Yang, L.; Wei, J.; Ma, K.; Gong, X.; Shang, J.; Yu, S.; Wang, F. An Autonomous Nonenzymatic Concatenated DNA Circuit for Amplified Imaging of Intracellular ATP. *Anal. Chem.* **2019**, *91* (23), 15229−15234.

(7) Wang, R.; Yu, L.; He, W.; Wu, Z.; Jiang, J. H. Chemically Inducible DNAzyme Sensor for Controllable Imaging of Metal Ions. *Anal. Chem.* **2024**, *96* (3), 1268−1274.

(8) Scalise, D.; Schulman, R. Controlling Matter at the Molecular Scale with DNA Circuits. *Annu. Rev. Biomed. Eng.* **2019**, *21*, 469−493.

(9) Li, J.; Macdonald, J.; Von Stetten, F. Review: A Comprehensive Summary of a Decade Development of the Recombinase Polymerase Amplification. *Analyst* **2019**, *144* (1), 31−67.

(10) Tian, W.; Li, P.; He, W.; Liu, C.; Li, Z. Rolling Circle Extension-Actuated Loop-Mediated Isothermal Amplification (RCA-LAMP) for Ultrasensitive Detection of MicroRNAs. *Biosens Bioelectron* **2019**, *128*, 17−22.

(11) Chen, Y.; Liu, Z.; Zhang, B.; Wu, H.; Lv, X.; Zhang, Y.; Lin, Y. Biomedical Utility of Non-Enzymatic DNA Amplification Reaction: From Material Design to Diagnosis and Treatment. *Small* **2024**, *20* (47), No. 2404641.

(12) Tang, L.; Luo, T.; Fan, S.; Liu, Y.; Song, J. Principles of Nucleic Acid Toehold Mediated Strand Displacement (TMSD) Reaction Model and Its Applications in Cell Environment. *Biomater Sci.* **2023**, *11* (15), 5060−5077.

(13) Li, S.; Zhu, L.; Lin, S.; Xu, W. Toehold-Mediated Biosensors: Types, Mechanisms and Biosensing Strategies. *Biosens Bioelectron* **2023**, *220*, No. 114922.

(14) Peng, H.; Newbigging, A. M.; Wang, Z.; Tao, J.; Deng, W.; Le, X. C.; Zhang, H. DNAzyme-Mediated Assays for Amplified Detection of Nucleic Acids and Proteins. *Anal. Chem.* **2018**, *90* (1), 190−207.

(15) Li, Y.; Luo, Z.; Zhang, C.; Sun, R.; Zhou, C.; Sun, C. Entropy Driven Circuit as an Emerging Molecular Tool for Biological Sensing: A Review. *TrAC Trends in Analytical Chemistry* **2021**, *134*, No. 116142.

(16) Dong, Z.; Su, R.; Fu, Y.; Wang, Y.; Chang, L. Recent Progress in DNA Biosensors for Detecting Biomarkers in Living Cells. *ACS Biomater. Sci. Eng.* **2024**, *10* (9), 5595−5608.

(17) Chan, H. N.; Ho, S. L.; He, D.; Li, H. W. Direct and Sensitive Detection of Circulating MiRNA in Human Serum by Ligase-Mediated Amplification. *Talanta* **2020**, *206*, No. 120217.

(18) Zhou, R.; Zeng, Z.; Sun, R.; Liu, W.; Zhu, Q.; Zhang, X.; Chen, C. Traditional and New Applications of the HCR in Biosensing and Biomedicine. *Analyst* **2021**, *146* (23), 7087−7103.

(19) Zhang, Q.; Su, C.; Qiu, J.-G.; Jiang, B.-H.; Zhang, C.-y. Advances in Enzyme-Free Nucleic Acid Amplification-Based Fluorescent Biosensors for Real-Time Imaging of DNA Repair Enzymes in Living Cells. *Coord. Chem. Rev.* **2023**, *496*, No. 215406.

(20) Chan, H. N.; Xu, D.; Ho, S. L.; He, D.; Wong, M. S.; Li, H. W. Highly Sensitive Quantification of Alzheimer's Disease Biomarkers by Aptamer-Assisted Amplification. *Theranostics* **2019**, *9* (10), 2939.

(21) Wu, Q.; Xu, W.; Shang, J.; Li, J.; Liu, X.; Wang, F.; Li, J. Autocatalytic DNA Circuitries. *Chem. Soc. Rev.* **2024**, *53* (22), 10878−10899.

(22) Wong, K. W.; Wang, Z.; He, D.; Li, H. W. Programmed Aptamer Target Chain Reaction (ATCR) for Smart Therapeutic Inhibitor Development. *Chem. Eng. J.* **2024**, *483*, No. 149228.

(23) Mo, L.; He, W.; Li, Z.; Liang, D.; Qin, R.; Mo, M.; Yang, C.; Lin, W. Recent Progress in the Development of DNA-Based Biosensors Integrated with Hybridization Chain Reaction or Catalytic Hairpin Assembly. *Front. Chem.* **2023**, *11*, No. 1134863.

(24) He, D.; Ho, S. L.; Chan, H. N.; Wang, H.; Hai, L.; He, X.; Wang, K.; Li, H. W. Molecular-Recognition-Based DNA Nanodevices for Enhancing the Direct Visualization and Quantification of Single Vesicles of Tumor Exosomes in Plasma Microsamples. *Anal. Chem.* **2019**, *91* (4), 2768−2775.

(25) Zhang, D. Y.; Turberfield, A. J.; Yurke, B.; Winfree, E. Engineering Entropy-Driven Reactions and Networks Catalyzed by DNA. *Science (1979)* **2007**, *318* (5853), 1121−1125.

(26) He, D.; Wang, H.; Ho, S. L.; Chan, H. N.; Hai, L.; He, X.; Wang, K.; Li, H. W. Total Internal Reflection-Based Single-Vesicle in Situ Quantitative and Stoichiometric Analysis of Tumor-Derived Exosomal MicroRNAs for Diagnosis and Treatment Monitoring. *Theranostics* **2019**, *9* (15), 4494.

(27) Steger, G.; Victor, J. Design of a DNAzyme: Prediction of MRNA Regions Accessible to a DNAzyme. *Methods Mol. Biol.* **2022**, *2439*, 47−63.

(28) Li, J.; Li, H. W. Ultrasensitive MiRNA Detection by AuNP-Based 3D DNA Walker and Catalytic Hairpin Assembly (CHA) Cascade Amplification for Early Cancer Diagnosis. *Chem. Asian J.* **2023**, *18* (15), No. e202300367.

(29) Wen, L.; Wang, M. Functionalities of PH-Responsive DNA Nanostructures in Tumor-Targeted Strategies. *J. Mater. Chem. B* **2024**, *12* (47), 12174−12190.

(30) Elbaz, J.; Shimron, S.; Willner, I. PH-Triggered Switchable Mg2+-Dependent DNAzymes. *Chem. Commun.* **2010**, *46* (8), 1209−1211.

(31) Han, Y.; Zhou, J.; Liu, F.; Ouyang, Y.; Yuan, R.; Chai, Y. Q. PH-Stimulated Self-Locked DNA Nanostructure for the Effective Discrimination of Cancer Cells and Simultaneous Detection and Imaging of Endogenous Dual-MicroRNAs. *Anal. Chem.* **2023**, *95* (34), 12754−12760.

(32) Han, Y.; Jiang, M.; Zhou, J.; Lei, H.; Yuan, R.; Chai, Y. The Acid-Stimulated Self-Assembled DNA Nanonetwork for Sensitive Detection and Living Cancer Cell Imaging of MicroRNA-221. *Anal. Chem.* **2024**, *96*, 16715.

(33) Guo, Y.; Yang, K.; Sun, J.; Wu, J.; Ju, H. A PH-Responsive Colorimetric Strategy for DNA Detection by Acetylcholinesterase Catalyzed Hydrolysis and Cascade Amplification. *Biosens Bioelectron* **2017**, *94*, 651−656.

(34) Cui, M. R.; Chen, Y.; Zhu, D.; Chao, J. Intelligent Programmable DNA Nanomachines for the Spatially Controllable Imaging of Intracellular MicroRNA. *Anal. Chem.* **2022**, *94* (30), 10874−10884.

(35) Greiner, J. V.; Glonek, T. Intracellular Atp Concentration and Implication for Cellular Evolution. *Biology (Basel)* **2021**, *10* (11), 1166.

https://doi.org/10.1021/prechem.4c00100
Precis. Chem. 2025, 3, 187−205

(36) Pellegatti, P.; Raffaghello, L.; Bianchi, G.; Piccardi, F.; Pistoia, V.; Di Virgilio, F. Increased Level of Extracellular ATP at Tumor Sites: In Vivo Imaging with Plasma Membrane Luciferase. *PLoS One* **2008**, *3* (7), No. e2599.
(37) Meng, X.; Dai, W.; Zhang, K.; Dong, H.; Zhang, X. Imaging Multiple MicroRNAs in Living Cells Using ATP Self-Powered Strand-Displacement Cascade Amplification. *Chem. Sci.* **2018**, *9* (5), 1184−1190.
(38) Liang, L.; Shuai, X.; Cao, L.; Wang, J.; Wang, Y.; Li, L.; Li, Y.; Huang, C.; Li, C. Endogenous Adenosine Triphosphate-Assisted Three-Dimensional DNA Walker Assembled on Soft Nanoparticles for Intracellular MicroRNA Imaging. *Anal. Chem.* **2023**, *95* (28), 10721−10727.
(39) Meng, X.; Wang, H.; Yang, M.; Li, J.; Yang, F.; Zhang, K.; Dong, H.; Zhang, X. Target-Cell-Specific Bioorthogonal and Endogenous ATP Control of Signal Amplification for Intracellular MicroRNA Imaging. *Anal. Chem.* **2021**, *93* (3), 1693−1701.
(40) Lei, H.; Zhou, J.; Liu, F.; Han, Y.; Chai, Y.; Yuan, R. A Fluorescence Light-Up 3D DNA Walker Driven and Accelerated by Endogenous Adenosine-5′-Triphosphate for Sensitive and Rapid Label-Free MicroRNA Detection and Imaging in Living Cells. *Anal. Chem.* **2024**, *96* (22), 9097−9103.
(41) Ortega, A. L.; Mena, S.; Estrela, J. M. Glutathione in Cancer Cell Death. *Cancers* **2011**, *3* (1), 1285−1310.
(42) Chen, T.; Wu, Q.; Cao, S.; Zhang, Q.; Isak, A. N.; Mao, D.; Lu, C.; Fu, X.; Feng, C.; Pan, Q.; Zhu, X. Nanodevice-Based Imaging of MiRNA in Vivo by Eliminating Blood Interference. *Chem. Eng. J.* **2022**, *430*, No. 132887.
(43) Wang, H.; Chen, Y.; Jiang, Y.; Wang, Y.; Li, R.; Shang, J.; Wang, F. Endogenous Glutathione-Activated Nucleic Acid Molecular Circuitry for Cell-Specific MicroRNA Imaging. *Anal. Chem.* **2024**, *96* (31), 12854−12861.
(44) Zhao, J.; Chu, H.; Zhao, Y.; Lu, Y.; Li, L. A NIR Light Gated DNA Nanodevice for Spatiotemporally Controlled Imaging of MicroRNA in Cells and Animals. *J. Am. Chem. Soc.* **2019**, *141* (17), 7056−7062.
(45) Zhao, X.; Zhang, L.; Gao, W.; Yu, X.; Gu, W.; Fu, W.; Luo, Y. Spatiotemporally Controllable MicroRNA Imaging in Living Cells via a Near-Infrared Light-Activated Nanoprobe. *ACS Appl. Mater. Interfaces* **2020**, *12* (32), 35958−35966.
(46) Zhou, H.; Jiang, Y.; Zhao, W.; Zhang, S. Light-Activated Nanodevice for On-Demand Imaging of MiRNA in Living Cells via Logic Assembly. *ACS Appl. Mater. Interfaces* **2022**, *14* (11), 13070−13078.
(47) Wang, C.; Xie, Y.; Song, X.; Chao, Z.; Wu, K.; Fang, Y.; Zhao, H.; Ju, H.; Liu, Y. A NIR Programmable In Vivo MiRNA Magnifier for NIR-II Imaging of Early Stage Cancer. *Angew. Chem., Int. Ed.* **2023**, *62* (50), No. e202312665.
(48) Hao, M.; Miao, P.; Wang, Y.; Wang, W.; Ge, S.; Yu, X.; Hu, X. X.; Ding, B.; Zhang, J.; Yan, M. Near-Infrared Light-Initiated Photoelectrochemical Biosensor Based on Upconversion Nanorods for Immobilization-Free MiRNA Detection with Double Signal Amplification. *Anal. Chem.* **2021**, *93* (32), 11251−11258.
(49) Ye, M.; Kong, Y.; Zhang, C.; Lv, Y.; Cheng, S.; Hou, D.; Xian, Y. Near-Infrared Light Controllable DNA Walker Driven by Endogenous Adenosine Triphosphate Forin SituSpatiotemporal Imaging of Intracellular MicroRNA. *ACS Nano* **2021**, *15* (9), 14253−14262.
(50) Xi, X.; Wu, Z.; Zhang, X.; Li, Y.; Zhao, Y.; Wen, W.; Wang, S. Endogenous Protease-Activatable Nanosensor Based on PNA-Peptide-DNA Engineering for AND-Gated and Dual-Model Detection of MicroRNA in Single Living Tumor Cells. *ACS Appl. Mater. Interfaces* **2023**, *15* (18), 21917−21928.
(51) Chen, B.; Qi, L.; Wu, Y.; Chen, M.; Zhou, Y.; He, L.; Zhang, B.; Zhang, M.; Wang, K.; He, X. Cell Membrane-Anchored AND Logic Gate Aptasensor for Tumor Cell-Specific Imaging with Improved Accuracy. *Anal. Chem.* **2024**, *96*, 14775.
(52) Green, S. J.; Lubrich, D.; Turberfield, A. J. DNA Hairpins: Fuel for Autonomous DNA Devices. *Biophys. J.* **2006**, *91* (8), 2966−2975.
(53) Chen, X.; Briggs, N.; McLain, J. R.; Ellington, A. D. Stacking Nonenzymatic Circuits for High Signal Gain. *Proc. Natl. Acad. Sci. U. S. A.* **2013**, *110* (14), 5386−5391.
(54) Zhu, Z.; Duan, X.; Li, Q.; Wu, R.; Wang, Y.; Li, B. Low-Noise Nanopore Enables In-Situ and Label-Free Tracking of a Trigger-Induced DNA Molecular Machine at the Single-Molecular Level. *J. Am. Chem. Soc.* **2020**, *142* (9), 4481−4492.
(55) Jiang, Y.; Li, B.; Chen, X.; Ellington, A. D. Coupling Two Different Nucleic Acid Circuits in an Enzyme-Free Amplifier. *Molecules* **2012**, *17* (11), 13211−13220.
(56) Zou, H.; Lin, C.; Zan, H.; Hu, Y.; Xu, X.; Wang, D.; Wang, Q.; Xie, Y.; Zhou, C. A Novel Fluorescent Aptasensor for Ultrasensitive Detection of Helicobacter Pylori in Stool Samples Based on Catalytic Hairpin Assembly Cascade Hybridization Chain Reaction. *Sens Actuators B Chem.* **2022**, *368*, No. 132157.
(57) Song, C.; Zhang, J.; Liu, Y.; Guo, X.; Guo, Y.; Jiang, X.; Wang, L. Highly Sensitive SERS Assay of DENV Gene via a Cascade Signal Amplification Strategy of Localized Catalytic Hairpin Assembly and Hybridization Chain Reaction. *Sens Actuators B Chem.* **2020**, *325*, No. 128970.
(58) Shi, J.; Song, Y.; Lin, Y.; Wu, Y.; Luo, H.; Yan, J.; Huang, K. J.; Tan, X. Sensitive Detection of Cancer Biomarker with Enzyme-Free Mediated Cascade Signal Amplification Empowered Undisturbed Dual-Mode Assay. *Sens Actuators B Chem.* **2023**, *394*, No. 134430.
(59) Dong, P.; Li, R.; He, S.; Zhang, Q.; Shang, J.; Jiang, Y.; Liu, X.; Wang, F. The Compact Integration of a Cascaded HCR Circuit for Highly Reliable Cancer Cell Discrimination. *Chem. Sci.* **2023**, *14* (8), 2159−2167.
(60) Chao, Q.; Zhang, Y.; Li, Q.; Jiao, L.; Sun, X.; Chen, X.; Zhu, L.; Yang, Q.; Shang, C.; Kong, R. M.; Fan, G. C.; Song, Z. L.; Luo, X. Compute-and-Release Logic-Gated DNA Cascade Circuit for Accurate Cancer Cell Imaging. *Anal. Chem.* **2023**, *95* (19), 7723−7734.
(61) Li, C.; Zhang, J.; Gao, Y.; Luo, S.; Wu, Z. S. Nonenzymatic Autonomous Assembly of Cross-Linked Network Structures from Only Two Palindromic DNA Components for Intracellular Fluorescence Imaging of MiRNAs. *ACS Sens.* **2022**, *7* (2), 601−611.
(62) Pan, J.; Deng, F.; Liu, Z.; Shi, G.; Chen, J. Toehold-Mediated Cascade Catalytic Assembly for Mycotoxin Detection and Its Logic Applications. *Anal. Chem.* **2022**, *94* (8), 3693−3700.
(63) Huang, Z.; He, D.; Li, H. W. A Fluorometric Assay of Thrombin Using Magnetic Nanoparticles and Enzyme-Free Hybridization Chain Reaction. *Microchimica Acta* **2020**, *187* (5), 1−8.
(64) Shen, Y.; Gong, J.; Li, S.; Liu, C.; Zhou, L.; Sheng, J.; Qingxia, X. Enzyme-Free Dual-DNA Walker Based on Catalytic Hairpin Assembled DNAzyme for Sensing Telomerase Activity. *Sens Actuators B Chem.* **2021**, *329*, No. 129078.
(65) Song, X.; Ding, Q.; Zhang, J.; Sun, R.; Yin, L.; Wei, W.; Pu, Y.; Liu, S. Smart Catalyzed Hairpin Assembly-Induced DNAzyme Nanosystem for Intracellular UDG Imaging. *Anal. Chem.* **2021**, *93* (40), 13687−13693.
(66) Li, B.; Jiang, Y.; Chen, X.; Ellington, A. D. Probing Spatial Organization of DNA Strands Using Enzyme-Free Hairpin Assembly Circuits. *J. Am. Chem. Soc.* **2012**, *134* (34), 13918−13921.
(67) Wei, J.; Gong, X.; Wang, Q.; Pan, M.; Liu, X.; Liu, J.; Xia, F.; Wang, F. Construction of an Autonomously Concatenated Hybridization Chain Reaction for Signal Amplification and Intracellular Imaging. *Chem. Sci.* **2018**, *9* (1), 52−61.
(68) Huang, D.; Li, X.; Shen, B.; Li, J.; Ding, X.; Zhou, X.; Guo, B.; Cheng, W.; Ding, S. Enzyme-Free Dual-Amplification Strategy for the Rapid, Single-Step Detection of Nucleic Acids Based on Hybridization Chain Reaction Initiated Entropy-Driven Circuit Reaction. *Sens Actuators B Chem.* **2018**, *273*, 393−399.
(69) Chen, H. J.; Hu, Y.; Yao, P.; Ning, D.; Zhang, Y. P.; Wang, Z. G.; Liu, S. L.; Pang, D. W. Accurate and Efficient Lipoprotein Detection Based on the HCR-DNAzyme Platform. *Anal. Chem.* **2021**, *93* (15), 6128−6134.
(70) Zhang, Y.; Li, R.; Yu, S.; Shang, J.; He, Y.; Wang, Y.; Liu, X.; Wang, F. Sensitive Autocatalytic Hybridization Circuit for Reliable In

Situ Intracellular Polynucleotide Kinase Imaging. *Anal. Chem.* **2022**, *94* (40), 13951−13957.
(71) Xiong, E.; Zhen, D.; Jiang, L. Homogeneous Enzyme-Free and Entropy-Driven Isothermal Fluorescent Assay for Nucleic Acids Based on a Dual-Signal Output Amplification Strategy. *Chem. Commun.* **2018**, *54* (89), 12594−12597.
(72) Xing, C.; Chen, Z.; Zhang, C.; Wang, J.; Lu, C. Target-Directed Enzyme-Free Dual-Amplification DNA Circuit for Rapid Signal Amplification. *J. Mater. Chem. B* **2020**, *8* (47), 10770−10775.
(73) Zhang, Q.; Zhao, R.; Li, C. C.; Zhang, Y.; Tang, C.; Luo, X.; Ma, F.; Zhang, C. Y. Construction of an Entropy-Driven Dumbbell-Type DNAzyme Assembly Circuit for Lighting Up Uracil-DNA Glycosylase in Living Cells. *Anal. Chem.* **2022**, *94* (40), 13978−13986.
(74) Zhou, Z.; Brennan, J. D.; Li, Y. A Multi-Component All-DNA Biosensing System Controlled by a DNAzyme. *Angew. Chem., Int. Ed.* **2020**, *59* (26), 10401−10405.
(75) Zhou, X.; Li, C.; Wang, W.; Zhang, F.; Zhou, Y.; Chen, D.; Wang, Z. DNAzyme Mediated Catalytic Hairpin Self-Assembly Strategy Enables the Sensitive and Facile Investigation of N6-Methyladenine. *Sens Actuators B Chem.* **2023**, *397*, No. 134665.
(76) Huang, X.; Li, Z.; Tong, Y.; Zhang, Y.; Shen, T.; Chen, M.; Huang, Z.; Shi, Y.; Wen, S.; Liu, S. Y.; Guo, J.; Zou, X.; Dai, Z. DNAzyme-Amplified Cascade Catalytic Hairpin Assembly Nanosystem for Sensitive MicroRNA Imaging in Living Cells. *Anal. Chem.* **2023**, *95* (31), 11793−11799.
(77) Zhu, D.; Hu, Y.; Xia, Y.; Wei, Y.; Lin, S.; Chao, J.; Su, S.; Wang, L. Non-Enzymatic Aptazyme-Driven Autonomous DNA Circuits Coupled with Three-Junction CHA for Amplified Live-Cell ATP Imaging. *Sens Actuators B Chem.* **2024**, *418*, No. 136259.
(78) Chen, H.; Song, J.; Li, Y.; Deng, D.; Song, Y.; Zhu, X.; Luo, L. Cascade Signal Amplifying Strategy for Ultrasensitive Detection of Tumor Biomarker by DNAzyme Cleaving Mediated HCR. *Sens Actuators B Chem.* **2024**, *420*, No. 136466.
(79) Wang, J.; Feng, Z.; Zhan, J.; Shi, Y.; Zhang, J. Ratiometric Detection of Lithium Ions in Serum and Living Cells Using DNAzyme-Assisted Hybridization Chain Reaction. *Sens Actuators B Chem.* **2024**, *410*, No. 135656.
(80) Wang, J.; Fu, X.; Liu, S.; Liu, R.; Li, J.; Wang, K.; Huang, J. Catalyst-Accelerated Circular Cascaded DNA Circuits: Simpler Design, Faster Speed, Higher Gain. *Small* **2023**, *19* (12), No. 2205903.
(81) Zhou, Z.; Lin, N.; Ouyang, Y.; Liu, S.; Zhang, Y.; Willner, I. Cascaded, Feedback-Driven, and Spatially Localized Emergence of Constitutional Dynamic Networks Driven by Enzyme-Free Catalytic DNA Circuits. *J. Am. Chem. Soc.* **2023**, *145* (23), 12617−12629.
(82) Liu, Y.; Shi, Y.; Wang, S.; Liu, S.; Shang, M.; Zhao, B.; Liu, H.; Yang, C.; Wang, F.; Kwok, C. K.; Wang, H. Hook-Like DNAzyme-Activated Autocatalytic Biosensor for the Universal Detection of Pathogenic Bacteria. *Anal. Chem.* **2024**, *96* (29), 11951−11958.
(83) Wang, X.; Liu, W. W.; Long, L. L.; Tan, S. Y.; Chai, Y. Q.; Yuan, R. Ultrasensitive Electrochemical Biosensor with Powerful Triple Cascade Signal Amplification for Detection of MicroRNA. *Anal. Chem.* **2024**, *96*, 15066.
(84) Wang, F.; Elbaz, J.; Teller, C.; Willner, I. Amplified Detection of DNA through an Autocatalytic and Catabolic DNAzyme-Mediated Process. *Angew. Chem., Int. Ed.* **2011**, *50* (1), 295−299.
(85) Qian, D.; Zhang, J.; Sun, G.; Zhang, Y.; Xu, Q.; Li, J.; Li, H. Programmable Entropy-Driven Circuit-Cascaded Self-Feedback DNAzyme Network for Ultra-Sensitive Fluorescence and Photoelectrochemical Dual-Mode Biosensing. *Anal. Chem.* **2024**, *96* (18), 7274−7280.
(86) Xing, C.; Lin, Q.; Gao, X.; Cao, T.; Chen, J.; Liu, J.; Lin, Y.; Wang, J.; Lu, C. Intracellular MiRNA Imaging Based on a Self-Powered and Self-Feedback Entropy-Driven Catalyst-DNAzyme Circuit. *ACS Appl. Mater. Interfaces* **2022**, *14* (35), 39866−39872.
(87) Gong, K.; Wu, Q.; Wang, H.; He, S.; Shang, J.; Wang, F. Autocatalytic DNAzyme Assembly for Amplified Intracellular Imaging. *Chem. Commun.* **2020**, *56* (77), 11410−11413.
(88) Zhang, Y.; Li, R.; Yu, S.; Shang, J.; He, Y.; Wang, Y.; Liu, X.; Wang, F. Sensitive Autocatalytic Hybridization Circuit for Reliable In Situ Intracellular Polynucleotide Kinase Imaging. *Anal. Chem.* **2022**, *94* (40), 13951−13957.
(89) Wang, Y.; Chen, Y.; Wan, Y.; Hong, C.; Shang, J.; Li, F.; Liu, X.; Wang, F. An Autocatalytic DNA Circuit Based on Hybridization Chain Assembly for Intracellular Imaging of Polynucleotide Kinase. *ACS Appl. Mater. Interfaces* **2022**, *14* (28), 31727−31736.
(90) Li, F.; Chen, Y.; Shang, J.; Wang, Q.; He, S.; Xing, X.; Wang, F. An Isothermal Autocatalytic Hybridization Reaction Circuit for Sensitive Detection of DNA Methyltransferase and Inhibitors Assay. *Anal. Chem.* **2022**, *94* (10), 4495−4503.
(91) Wei, J.; Wang, H.; Wu, Q.; Gong, X.; Ma, K.; Liu, X.; Wang, F. A Smart, Autocatalytic, DNAzyme Biocircuit for in Vivo, Amplified MicroRNA Imaging. *Angew. Chem., Int. Ed.* **2020**, *59* (15), 5965−5971.
(92) Li, R.; Zhu, Y.; Gong, X.; Zhang, Y.; Hong, C.; Wan, Y.; Liu, X.; Wang, F. Self-Stacking Autocatalytic Molecular Circuit with Minimal Catalytic DNA Assembly. *J. Am. Chem. Soc.* **2023**, *145* (5), 2999−3007.
(93) Wei, J.; Yu, M.; Tan, K.; Shang, J.; He, S.; Xie, C.; Liu, X.; Wang, F. Tailoring a Minimal Self-Replicate DNA Circuit for Highly Efficient Intracellular Imaging of MicroRNA. *Small* **2023**, *19* (17), No. 2207961.
(94) Wei, J.; Shang, J.; He, S.; Ouyang, Y.; Willner, I.; Wang, F. Construction of a Homogeneous Enzyme-Free Autocatalytic Nucleic Acid Machinery for High-Performance Intracellular Imaging of MicroRNA. *CCS Chem* **2022**, *4* (11), 3549−3562.
(95) Wang, H.; He, Y.; Wei, J.; Wang, H.; Ma, K.; Zhou, Y.; Liu, X.; Zhou, X.; Wang, F. Construction of an Autocatalytic Hybridization Assembly Circuit for Amplified In Vivo MicroRNA Imaging. *Angew. Chem., Int. Ed.* **2022**, *61* (19), No. e202115489.
(96) Wan, Y.; Li, G.; Zou, L.; Wang, H.; Wang, Q.; Tan, K.; Liu, X.; Wang, F. A Deoxyribozyme-Initiated Self-Catalytic DNA Machine for Amplified Live-Cell Imaging of MicroRNA. *Anal. Chem.* **2021**, *93* (31), 11052−11059.
(97) Yin, P.; Choi, H. M. T.; Calvert, C. R.; Pierce, N. A. Programming Biomolecular Self-Assembly Pathways. *Nature* **2008**, *451* (7176), 318−322.
(98) Gao, Y.; Fan, X.; Zhang, X.; Guan, Q.; Xing, Y.; Song, W. HCR/DNAzyme-Triggered Cascaded Feedback Cycle Amplification for Self-Powered Dual-Photoelectrode Detection of Femtomolar HPV16. *Biosens Bioelectron* **2023**, *237*, No. 115483.
(99) Han, Y.; Li, D. L.; Han, Q.; Ma, F.; Zhang, C. Y. Integration of Demethylation-Activated DNAzyme with a Single Quantum Dot Nanosensor for Sensitive Detection of O6-Methylguanine DNA Methyltransferase in Breast Tissues. *Anal. Chem.* **2024**, *96* (11), 4487−4494.
(100) Shi, H.; Zheng, J.; Wang, Y.; Zhu, S.; Xiang, Y.; Zhu, X.; Li, G. Point-of-Care Testing of Protein Biomarkers by Integrating a Personal Glucose Meter with a Concatenated DNA Amplifier. *Sens Actuators B Chem.* **2020**, *322*, No. 128659.
(101) Gong, X.; Li, R.; Wang, J.; Wei, J.; Ma, K.; Liu, X.; Wang, F. A Smart Theranostic Nanocapsule for Spatiotemporally Programmable Photo-Gene Therapy. *Angew. Chem.* **2020**, *132* (48), 21832−21839.
(102) Xiao, M.; Lai, W.; Wang, F.; Li, L.; Fan, C.; Pei, H. Programming Drug Delivery Kinetics for Active Burst Release with DNA Toehold Switches. *J. Am. Chem. Soc.* **2019**, *141* (51), 20354−20364.

https://doi.org/10.1021/prechem.4c00100
Precis. Chem. 2025, 3, 187−205